

YEAR 2

**DEVELOPMENT OF PERMEABLE REACTIVE BARRIERS  
FOR CHROMIUM RESIDUE SITES IN NEW JERSEY**

**Final Report**

**By**

**M. E. Labib, S. S. Dukhin and J. Schuring  
New Jersey Institute of Technology  
Newark, NJ 07102**

**Submitted to:**

**Dr. Paul Sanders  
New Jersey Department of Environmental Protection  
Division of Science, Research & Technology  
Trenton, NJ 08625**

**November 12, 1999**

## Executive Summary

1. The reactive media capacities (RMC) of four reactive irons, iron-pyrite and iron-siderite mixtures were evaluated by the "thin plug" method developed at NJIT. The RMC of iron at high pH is very low and has been found to be insufficient for use in PRB for the case of NJ sites. The RMC of iron-pyrite and iron-siderite mixtures were found to be more than 10 times larger than that of conventional reactive iron. The levels of reactive capacities of the mixture developed in this study are sufficient for installing PRB for the Allied Signal and P.P.G. sites. However, because of the high Cr concentration and high flow rates of the C.L.H. site, a rather large barrier thickness (3-4m) would be necessary. This site requires an exceptionally high reactive capacity of about  $100 \text{ mg/cm}^3$ . Other barrier designs suitable for the latter site have been evaluated during this research. These are summarized below.
2. Measuring the dependence of RMC on RM nature, chromium concentration, GW velocity and residence time was made possible by the use of the new "thin plug" requiring only 3 months duration. Because of this new development, it has been possible to accomplish these results by conducting 15 parallel experiments exploring most of the variables affecting the RMC. This new thin RM plug method simplifies the experimental verification of the parameters needed to perform long-term assessment of the barrier needed for this application.
3. The comparison of RMC measured in the laboratory with the barrier critical capacity (the entire chromium amount accumulated per  $1 \text{ cm}^3$  of a barrier surface area due to groundwater crossing the barrier during its entire life) enabled us to calculate the critical thickness,  $d_{bc}$  for the barrier. If the predicted critical thickness of a barrier is not too large, the suitability of the RM for a successful barrier installation can be made after accounting for HC issues pertaining to various sites. This simple approach to determine the barrier critical thickness assumes a uniform distribution for accumulated chromium within the barrier. Dynamic models for chromium accumulation within the barrier as a function of time and of distance to barrier front surface have been elaborated. Combination of the results of these models with the measurements of chromium reduction kinetics in the laboratory has confirmed the validity of the assumption about the uniform chromium distribution as first approximation.
4. A complete analysis of the mode of groundwater flow and the possibility of bypassing was performed and characterized by the hydraulic conductivities of various parts of the landscape. There is a convergent GW flow before waste depository if its hydraulic conductivity,  $K_w$  exceeds that of surrounding soil,  $K_s$ . The capture width and correspondingly barrier critical thickness can double at large  $K_w$  condition. There is a divergent flow before WD, if  $K_w < K_s$ . The capture width and correspondingly  $d_{bc}$  decrease proportional to  $K_s$ . The measurement of  $K_w/K_s$  ratio for every WD (site) is important. A method for this measurement is proposed with account for information about hydrodynamic field around a waste depository.

5. The barrier critical thickness for Allied Signal, P.P.G. and C.L.H. sites are correspondingly less than 1m, 1m and 5m for 20 years of barrier work if the filling material is the RM only – i.e., iron-pyrite mixture for example. However, the RM mixing with soil (sand) is necessary to eliminate bypassing due to the decrease in hydraulic conductivity of RM due to chromium accumulation and calcium deposit formation; this decrease can be about as much as a factor of 10. The mixing of RM at volume fraction of 0.2 with coarse sand is proposed to avoid bypassing. As a result, the barrier critical thickness would increase 5 times; the thickness of the barrier becomes 1-2m for the Allied Signal site and 3-4 m for the P.P.G. site. The above prediction is not very reliable if soil conductivity is high and mixing with RM causes a large decrease in HC and correspondingly causes the bypassing. The use of very coarse sand may not be appropriate because the small pyrite particle can fall through the broad pores between the coarse sand particles and the top portion of the barrier can lose a portion of the RM. Nevertheless, our analysis still shows that the application of the conventional barrier technology using RM/sand mixing is suitable for the Allied Signal site. This is because the RM fraction needed in this case is small and will not be accompanied with a significant decrease in HC and thus only very weak bypassing would occur.
6. For the P.P.G site, four scenarios can be proposed, depending on the  $K_w$  and  $K_s$  values in the site; this situation will be evaluated after receiving the accurate information about this site. The four scenarios are as follows:
- If  $K_w < K_s$  and  $K_s$  is not large, perhaps the conventional RM/sand mixing is suitable.
  - If  $K_s$  is not low, the conventional RM and soil mixing would cause the mixture's HC to decline which causes  $K_{RM}$  to decline with chromium accumulation and cause GW bypassing. For the prevention of bypassing, a two-step technology has to be applied. First a small fraction has to be removed from the soil before mixing or coarse sand fraction has to be used. The optimal soil (sand) fraction (Section 2.5) has to be determined and used that will increase the  $K_{mix}$  value. As this compensation will not be sufficient, i.e. if  $K_{mix}(p_{opt}) < K_s$ , the bypassing is not avoidable. If it will be so, the optimal weak mixing has to be investigated and specified for the P.P.G. soil; this will suppress  $K_{mix}$  decline with chromium accumulation (Section 2.8).
  - At  $K_w > K_s$ , the critical barrier capacity and  $d_{bcr}$  can increase twice, i.e.  $d_{bcr} = 8 - 10m$  at  $p_{opt} = 0.2$  (Section 2.10). A reasonable barrier thickness less than 4m can be provided with  $p_{opt} \sim 0.4-0.5$ . At this large  $p_{RM}$ , the possibility of preventing  $K_{mix}$  decline with RM aging using optimal weak mixing is questionable. The prevention of bypassing at  $p_{opt} \sim 0.5$  and consequently providing  $d_{bcr} \sim 4m$  at the most unfavorable conditions, namely at  $K_w > K_s$  and large  $K_s$  is possible with the use of the proposed layered RM/soil (sand) structure (Section 2.9). The layered RM/sand structure deserves attention as an option if it turns out that  $K_w < K_s$  and  $K_s$  is not so large in the P.P.G. case, since a large  $p_{RM}$  can be used and a smaller  $d_{bcr}$  is sufficient. The identification of the P.P.G. conditions ( $K_w$ ,  $K_s$ ) as one among the above 3 cases and the RM/sand technology specification for the P.P.G. site will be possible if  $K_w$  and  $K_s$  measurements and long term investigation of  $K_{mix}$  decline with time become available.
  - The application of the "reactive filter" technology (Section 5), i.e. PRB with channels incorporated in RM is the most reliable technology for the P.P.G. site. The additional cost due to channel incorporation can be compensated by the smaller barrier thickness.  $d_{bcr} \sim 1m$  will be possible with the use of reactive filter as compared to  $d_{bcr} \sim 4m$

using the conventional RM/sand technology. In the case of the reactive filter, a high volume fraction for RM is possible (about 0.9) and therefore, a large decrease in its critical thickness would be possible in all the cases.

7. For the Chemical Land Holding site, a reasonable barrier thickness (4m) is possible if the RM volume fraction exceeds 0.8-0.9. Perhaps the only PRB technology that can provide such a high RM volume fraction is the reactive filter described in this report. Geo-textiles are reliable and cheap materials for the channel realization within RM. The smaller the number of channels,  $n$  per 1m of barrier length, the simpler and cheaper would be the reactive filter needed for this treatment. The larger the values of  $K_s$  and  $K_w$ , the larger the number,  $n$ . The number of channels and reactive filter specification for the C.L.H. site will be possible after the specific values of  $K_s$  and  $K_w$  are obtained.
8. In parallel with Cr(III) accumulation on the RM particles surface, calcium carbonate deposit formation or other mineral precipitation can decrease the pore cross-sections of mixture in the barrier; this is accompanied with decline of HC of RM or RM/soil mixture. In the case of the iron-pyrite mixture, the HC decline can be further enhanced because the pores between pyrite particles are smaller. The smaller the pores, the stronger will be their clogging by deposit formation. A "coarse" gravel layer on upstream side of barrier can be arranged so that deposit formation would take place first on the coarse particles; clogging the broad pores between coarse particles is difficult. The mineral precipitation in this coarse gravel layer decreases the  $Ca^{++}$  concentration and consequently suppresses the mineral precipitation within subsequent RM layer. This method of suppression of mineral precipitation has to be used in parallel with HC decline suppression by using optimized weak mixing etc. Large gravel dimension is favorable to decrease the clogging of pores between gravel particles. Thus an optimal gravel (sand) particle dimension exists which provides larger specific surface for mineral precipitation and in parallel excludes the clogging of not too small pores.

## Introduction

Reactive media mixtures having high reduction capacities have been developed for use in permeable barriers to treat high pH Cr-contaminated groundwater, as in the case of Cr sites in New Jersey. As previously discussed, the passivation of the iron reactive medium at the high pH condition is the main obstacle in applying the reactive barrier technology for the New Jersey sites. In this case, passivation is manifested by a decrease in the reduction rate as a function of Cr (III) accumulation on the surface of iron particles. There is no available data, experimental techniques or documentation in the literature for quantifying or characterizing the kinetics of this passivation phenomenon, especially in terms of the decrease in the reaction rate constant as a function of time in the barrier. Section 1 includes an account of our experimental investigation of passivation kinetics along with results and analysis of the phenomenon, as they pertain to the reactive barrier problem.

Since a significant decrease in hydraulic conductivity (HC) of reactive media (RM) was found to take place during chromium accumulation, a large attention was paid to understanding and optimizing the entire barrier system. The optimization of HC-related issues included the use of the conventional method of mixing the RM with soil or sand – these results are given in Section 2. Because of the significant implication of the decrease in HC on groundwater bypassing around the barrier, this process was modeled in detail (Section 3). The results of this optimization indicates that a conventional barrier with sufficient barrier reactive capacity and high HC can be designed for the Allied Signal and P.P.G. sites, but not for the Chemical Land Holding (CLH) site. The CLH site is expected to require a much larger reactive capacity, and correspondingly a large barrier thickness, especially if RM/sand mixture is used in construction.

Based on our analysis, the large barrier capacity and high HC requirements for the CLH site cannot be satisfied by using the conventional RM/sand permeable barrier having a reasonable thickness. To overcome this and related limitations, a new technology (reactive filter) was developed. This reactive filter technology is expected to provide an effective barrier with HC 100 - 1000 times higher that of conventional trench-filled technology, and with effective reactive capacity.

### 1. Capacities of a Reactive Media and a Barrier

1.1. It is well known in the literature that at lower and moderate pH, higher reduction rates of Cr(VI) can be achieved with iron powder as reactive media [1-10]. In our experiments, an initial (early in time) high reduction rate with iron could be measured, even at the high pH condition, about 11.5. However, at this high pH, and with a small accumulation of chromium, the reduction rate decreases very rapidly. Based on these reaction rates, the remediation of the three sites of Hudson County using iron as the only reactive media is impossible (Figs. 1-2). To overcome the above limitation, we studied iron-pyrite [11-12] and iron-siderite mixtures as RM (Figs. 3-7). A thin layer column (plug) consisting of an iron-pyrite mixture results in the accumulation of Cr(III) up to 20 mg/cm<sup>3</sup> in a 3-months experiment. In evaluating these results, the residence time (time available for reduction of a groundwater volume moving through a barrier) is important. The residence time is defined as the ratio of barrier thickness to GW velocity. By analogy, in our experiments this residence time is the thickness of used iron plug containing RM to filtration velocity.

Usually, the column (plug) length in our experiments is equivalent to the barrier thickness. In situations when the reduction rate of the contaminant is low, long residence time and large column length are necessary to provide effluent concentration,  $n_{eff}$  much smaller than influent concentration,  $n_{in}$ . However, in the case of chromium, the reduction rate is rather high even at pH = 12. With reduction coefficient,  $K_{red}$  of 7 cm/hour, a small residence time of 30 minutes is sufficient for effecting a complete reduction with a column length of 3 cm and at a velocity of 6 cm/hr (150 cm/day). The flow rates (velocities) for the three sites of Hudson County are almost 10 times smaller. Thus, a small column with RM layer thickness of 3-4 cm was sufficient to achieve the results needed in our experimental work (Fig. 8). Moreover, in our experiments, the residence time was smaller and the velocity was higher than for barrier, i.e. conditions were more difficult for reduction.

The use of small columns is advantageous, especially for long-term prognosis of barrier performance. In our experiments, one column provided the chromium reduction for a period of 3 months. Since a barrier thickness of 100 cm is 30 times larger than RM layer thickness in a small column, the barrier can be modeled as a series of 30 small columns. This series of 30 columns will reduce and accumulate chromium 30 times larger, i.e. simulating a period of 90 months. It means that a barrier active life of 90 months can be predicted using the experimental data for 3 months' performance of a small column, if the velocity is same in both the cases. Therefore, the prognosis for 20 years' performance can be made in our experiment if the filtration velocity is increased three-folds than that of the barrier. Because of the very long duration of the experiment, we have been performing 15 small column experiments in parallel for 3 months or more. Thus, the role of many parameters (RM nature, flow rate, GW type etc.) can be investigated in a reasonable time.

1.2. The reduction rate of chromium ( $Cr^{6+}$ ) during 3 months experiments was measured by using groundwater of C.L.H. and P.P.G. with influent concentrations,  $n_{in}$  of 55 ppm and 16 ppm, respectively. The effluent concentration,  $n_{eff}$  and the amount of chromium accumulated in 1 cm<sup>3</sup> of RM (reactive capacities) are shown in Figs. 3-7. The figures show that the effluent concentration increases with the accumulation of chromium in the column. The increase in effluent concentration causes a decrease in the reduction rate. These experiments enabled us to determine the maximum amount of chromium accumulated in 1 cm<sup>3</sup> of RM (RM capacity).

Table 1. Capacity of reactive media (chromium amount accumulated in 1 cm<sup>3</sup> of RM during 3 months)

Experiment	RM*	Capacity (mg/cm <sup>3</sup> )
1	Pyrite/iron 3	20
2	Pyrite/iron 3	16
3	Pyrite/iron 3	17
4	Pyrite/iron 2	20
5	Pyrite/iron 3	20

\* Four kinds of iron were used in experiments without pyrite and only two kinds were used in experiments with pyrite. These two kinds (iron 2 and iron 3) were chosen because they achieved large reduction rates. The initial reduction rate was higher for iron 2. However, the specific surface area for iron 3 far exceeds that of iron 2 (Appendix 1).

### 1.3. Flow Rate Influence on RM Capacity

The two curves shown in Fig. 7 correspond to different flow rates and demonstrate the difference in performance between two iron-pyrite mixtures. The increase in flow rate of groundwater through the column by approximately 10 times is accompanied by a decrease in RM capacity of 15-20 times i.e. 1 mg/cm<sup>3</sup> instead of 20 mg/cm<sup>3</sup>. This can be interpreted if we account for the competition between two processes -- passivation and regeneration. In parallel with Cr(III) accumulation on the iron particle surface, which decreases a part of surface available for reduction, an opposite process takes place which regenerates the reduction ability of such surface. To illustrate these effects, the chromium reduction is accompanied with the formation of a surface compound containing Fe<sup>3+</sup> [4]. Beneath this compound, Fe<sup>0</sup> is present which in turn reduces Fe<sup>3+</sup> into Fe<sup>2+</sup>. The Fe<sup>2+</sup> formation enhances the particle ability to reduce chromium because Fe<sup>2+</sup> is an electron donor. Also, the simultaneous corrosion processes occurring during the reaction are expected to be involved in the regeneration process; this process has not been investigated.

The slower the reduction process, the stronger is the rate of regeneration process. At higher Cr<sup>6+</sup> concentration, the reduction rate is higher and the rate of regeneration is lower and thus cannot compete with reduction – i.e. the role of the regeneration process is minor in this case. At lower Cr<sup>6+</sup> concentration, the reduction rate is lower and the regeneration can compete with reduction. The latter can be observed by comparing the results of 55 ppm versus 16 ppm Cr concentration in groundwater.

Since the linear velocity of groundwater influences the RM capacity, velocities similar to those present within a barrier were used in our small column experiments, i.e. velocities in the range of 0.1-1.0 cm/hr were used to assess the realistic situation occurring in the barrier.

1.4. By using the measured RM capacity, we can find out whether iron-pyrite mixture can provide the barrier work for 5-20 years at pH = 12. This is done by comparing the amount of chromium that enters the barrier with the GW stream,  $C_{bcr}$  and the amount of chromium that can be reduced within the barrier. The amount  $C_{bcr}$  is proportional to chromium concentration in GW,  $n_i$ , GW stream velocity,  $u$  and time,  $T_b$  of barrier work, i.e.

$$C_{bcr} = n_i u T_b \quad (1.1)$$

$C_{bcr}$  is the critical barrier capacity, i.e. the entire chromium amount per 1 cm<sup>2</sup> of barrier surface area, which crosses the barrier during time  $T_b$  and has to be reduced. This amount flows through a unit surface area of the barrier and has to be accumulated in a volume proportional to its thickness,  $d_b$ , i.e.

$$n_i u T_b = c_{bcr} d_b \quad (1.2)$$

This equation determines a barrier's specific critical capacity,  $c_{bcr}$  (mg/cm<sup>3</sup>) at a given  $d_b$  value.

### 1.5. The Demands to the RM Capacity

The requirements for the RM capacity,  $c_{RM}$ , namely the condition:

$$c_{RM} > c_{bcr} \quad (1.3)$$

is necessary for a barrier work, where  $c_{bcr}$  relates to a definite  $d_b$  value. Equation (1.2) is used for calculating the critical capacities for the three sites using information about the chromium concentration in GW, velocity of GW and for  $d_b = 1$  m. The specification of critical barrier

capacity,  $C_{bcr}$  is necessary for a more complete account of GW stream within a site (Appendix 2).

Table 2. Concentration, GW velocity and barrier capacity of the three sites

	C.L.H.		Allied Signal		P.P.G.					
Concentration (ppm)	55		25		16					
GW velocity (ft/d)	0.17 f/d*	0.84 f/d	13 f/y**	35 f/y	0.5 f/d					
GW velocity (cm/day)	5.2	26	1.1	3	15.2					
Barrier life (years)	5	20	5	20	5	20				
Barrier capacity (mg/cm <sup>3</sup> )	5	20	25	100	0.5	2	1.4	5.4	4.4	17

\* - feet/day    \*\* - feet year

The choice between iron-pyrite and iron-siderite mixtures is accomplished on the basis of their solubilities in water (Appendix 3). The siderite solubility is so high that it will dissolve in GW stream in less than 20 years. The comparison of data in Tables 1 and 2 shows that iron-pyrite capacity is sufficient for all sites with the exception of the C.L.H. site for a duration of 20 years; a barrier may be possible for 5 to 10 years.

## 2. Barrier Design and Prevention of Groundwater Streamlining

### 2.1. Hydraulic Conductivities of Soil and RM

The HC of fresh iron-pyrite mixture was measured and was found to be lower than that of iron. This is because pyrite particle size is smaller than that of iron. In Table 3, iron-pyrite HC,  $K_{ip}$  and the range for soil HC,  $K_s$  at different points of Allied Signal site are given. Initially, the difference between  $K_{ip}$  and  $K_s$  is not very large. This conclusion changes as HC measurement was made after chromium accumulation inside the reactive medium. With the accumulation of chromium, HC decreases 10 times. Due to this strong decrease in HC, the problem of GW streamlining around the barrier arises, and must be considered in detail for the design of a practical barrier.

Table 3. HC of site soil, and iron-pyrite mixture – both fresh and after prolonged use in Cr reduction

Powder	HC (ft/day)
Site soil	1 - 19
Iron 3/pyrite mixture, fresh	2.0
Iron 3/pyrite mixture, 3 months of work	0.2

The decrease in HC can be explained by two possible mechanisms, namely: specific and nonspecific [13]. The specific mechanism pertains to the accumulation of Cr as the reduction

proceeds with time, as well as the deposition of other compounds such as calcium carbonate during the process. The accumulated chromium compounds occupy a large volume on material that decreases the dimensions of pores between particles and causes a decrease in HC. Also, the deposition of non-soluble salts of  $\text{Ca}^{++}$  can also decrease the HC during the groundwater flow in the barrier [13]. At the same deposition rate, the smaller the pores, the larger will be the HC decline by the above mechanism. The nonspecific process refers to the particle dimensions and other geometrical variables of particles inside the barrier. For example, the pyrite particles are small and can intensify the HC decline. This issue will be addressed in a separate section in more detail.

## 2.2. GW Streamlining Around the Barrier and Its HC

When the barrier hydraulic conductivity,  $K_b$ , is equal to the aquifer hydraulic conductivity,  $K_a$ , the GW stream is not deformed by the barrier, i.e. GW trajectories are straight lines. Any small decrease in  $K_b$  in comparison with  $K_a$  retards the GW stream and causes streamlining around the barrier. The smaller the difference between the above hydraulic conductivities, the smaller is the streamlining. In Appendix 4, it is shown that the streamlining is almost negligible even if  $K_b$  is 2-3 times smaller than  $K_a$ . Thus the condition:

$$K_b > 0.3K_a \quad (2.1)$$

is a necessary condition for a barrier design (Fig. 9). If  $K_b$  decreases with chromium accumulation then condition (2.1) has to be satisfied.

## 2.3. Using RM or RM/Soil Mixture as Barrier Installation

If HC of RM is much smaller than that of aquifer, a mixture of aquifer soil with RM is conventionally prepared and used as the reactive mixture for the barrier. The values of these mixtures' hydraulic conductivity,  $K_{mix}$  will be between the values of HC of RM,  $K_{ip}$  and HC of aquifer,  $K_s$ , i.e.

$$K_{ip} < K_{mix} < K_s \quad (2.2)$$

The smaller the RM volume fraction,  $p$ , the smaller will be the difference between  $K_{mix}$  and  $K_s$ . In our case the waste HC plays an additional role, as well.

## 2.4. GW Stream Around and Within Waste Depository and Relation to PRB Design

The three sites of Hudson County are considered as waste depositories, and this may create a large specificity in the optimization of barrier design, and its HC condition requirements. In addition to  $K_s$  and  $K_{RM}$ , the hydraulic conductivity of waste,  $K_w$  has to be taken into account. The difference between  $K_w$  and  $K_s$  complicates the GW flow field even in the absence of a barrier. The account for the regional hydraulic gradient value is not sufficient for characterizing GW flow field in this case.

The GW steady flow field before a barrier installation has to be properly characterized to choose the barrier geometry and to analyze the possibility of streamlining around it. If the shape of waste depository is isometrical, i.e. its linear dimension difference in different directions is not large, it can be considered as circular. In this case, a depository can be characterized with its radius  $R$  and hydraulic conductivity,  $K_w$ . The exact mathematical description of flow field is possible in this case (Appendix 5). Three qualitative different cases can be discriminated:

$$K_w = K_s \quad (2.3)$$

$$K_w < K_s \quad (2.4)$$

$$K_w > K_s \quad (2.5)$$

The water field is characterized by straight lines in the first case (Fig. 10a). If  $K_w = 0$ , i.e. a depository is not permeable for GW flow then streamlining takes place. The streamlining around a depository takes place as  $K_w$  is nonzero but small in comparison with  $K_s$ . In this case GW mainly streamlines around the depository and a small part of stream penetrates inside it. It means the flow upstream is divergent and downstream is convergent (Fig. 10b). In the third case, the conditions for GW flow into depository are favorable. The flow upstream of depository is convergent and downstream of it is divergent (Fig.10c). In Appendix 5, the flow field is quantified.

The coordinate  $x$  in the direction of regional hydraulic gradient,  $u_e$  and the circular coordinates  $r$ ,  $\theta$  with center at depository's center ( $r = 0$ ) are introduced. The angles,  $\theta = 0$  and  $\theta = \pi$  correspond to front and back poles of the depository and  $\theta = \pi/2$  corresponds to its equator. The total stream of GW into a depository is obtained by integrating over its boundary in the range  $0 < \theta < \pi/2$  (Appendix 5).

$$Q = \pi R u \frac{2K_w}{K_w + K_s} \quad (2.6)$$

For condition (2.3),  $Q$  can be calculated as unidirectional flow through the circular area,  $\pi R^2$  as:

$$Q_{||} = \pi R^2 u \quad (2.7)$$

The same result follows from more general equation (2.6) that simplifies at condition (2.3). It can be seen that at condition (2.4):

$$Q < Q_{||} \quad (2.8)$$

and at condition (2.5):

$$Q > Q_{||} \quad (2.9)$$

$Q$  growth with increasing  $K_w$  is restricted by the maximum value corresponding to:

$$K_w \gg K_s \quad (2.10)$$

This maximum value is twice larger than  $Q_{||}$ .

The specific GW flow field within the depository causes the necessity to specify the equation for the entire barrier capacity. It can be seen from equation (2.6) that at the same value of the regional hydraulic gradient, i.e. at the same  $Q_{||}$ , the entire stream through the barrier can be larger or smaller than  $Q_{||}$ , namely larger not more than twice and as small as  $K_w$  is small in comparison with  $K_s$ . Thus the multiplier has to be introduced in equation for entire barrier reactive capacity (1.1):

$$C_b = \frac{2K_w}{K_w + K_s} u_s n_i \quad (2.11)$$

The second conclusion is that the barrier needs to comprise the entire back boundary of depository, namely the arc (Fig. 10)

$$r = R, \quad \frac{\pi}{2} < \theta < \pi \quad (2.12)$$

## 2.5. Importance of RM Mixing with Monodisperse Fraction of Sand (Soil) for Bypassing Prevention

The mixing with coarse sand was used [14] to provide larger HC of barrier and to prevent bypassing. Coarse sand was used rather than the aquifer material to insure that the permeability of the wall would be at least as high as that of the surrounding aquifer. The HC values of native sand and sand/iron mixture were measured as  $7.24 \times 10^{-3}$  cm/sec and  $4.37 \times 10^{-2}$  cm/sec, respectively. The larger the sand porosity, the larger will be the space available for RM to occupy pores in soil (sand). It is well known in the literature that the porosity of monodisperse powder consisting of spherical particles is 0.4-0.5. In polydisperse sand, porosity decreases because smaller particles occupy space between larger ones (Fig. 11). Thus fractionating the soil (sand) may enable us to increase RM volume fraction with the preservation of pores for water movement.

The larger the monodisperse fraction dimension, the larger will be the pores for water transport at the same RM volume fraction. However, our experiments demonstrated a difficulty that excludes the possibility of using too coarse fractionated sand. It turned out in experiments with monodisperse glass beads (1mm diameter) that RM falls down through thick pores between beads (gravitational segregation). It is well known that pores between monodisperse spherical particles approximately equals 0.2-0.4 of diameter. It means in this case pores of 200  $\mu$ m are available which are larger than the dimensions of majority of the particles in iron-pyrite mixture. Thus, the smaller fraction of sand namely 300-500 micron has to be used with pores between particles smaller than iron-pyrite dimensions (50-100 micron).

The situation can change if the iron-pyrite mixture is aggregated because these aggregates do not fall through the small pores. The aggregate sticking to the sand surface can prevent the gravitational segregation as well. However, the aggregation and sticking are sensitive to electrolytic nature and content. As GW chemistry changes, the disaggregation and detachment can occur. The gravitational segregation in a barrier is not admissible because its upper part could loose RM due to sedimentation that will be a serious damage to the barrier and to the effectiveness of the treatment.

We can conclude that an optimal monodisperse fraction of coarse sand exists for mixing with RM. Very large monodisperse particles cannot be used because of the gravitational segregation. Very small monodisperse particles cannot be used because the mixture HC will be small. The optimal fraction is the largest fraction among other fractions for which RM gravitational segregation is impossible. The bypassing will be absent if:

$$K(p_{opt}) > K_s \quad (2.13)$$

In the opposite case, bypassing takes place that will be considered in Section 3.

The experimental determination of the optimal volume fraction,  $p_{opt}$  of RM and its hydraulic conductivity,  $K(p_{opt})$  is an important task. The necessity of long-term investigations has to be emphasized because the initial HC can be rather large. If HC of RM in pores between larger sand particles will decrease 10 times, as it was found in pure RM case, a strong decrease of  $K(p_{opt})$  in time is possible. This possible harmful phenomenon has to be examined for long-

term investigations.

### *2.6. Low Conductivities of Depository Waste and Soil as the Main Conditions for the Suitability of RM/Sand Mixture for a Barrier Installation*

In comparison to the conventional case of using iron for RM, the additional use of pyrite will cause a decrease in  $K(p_{opt})$ . This is because the smaller the RM particles the smaller will be the dimension of optimal sand fraction. Their decrease will cause a strong decrease in  $K(p_{opt})$  value. As a result, the main condition (2.13) necessary for the absence of bypassing is satisfied in this case as both  $K_s$  and  $K_w$  are rather small. In the opposite case, the bypassing can be a serious restriction for RM/sand mixture application for barrier installation. It means the experimental determination of  $K(p_{opt})$ ,  $K_w$  and  $K_s$  is an important prerequisite to evaluate the suitability of RM/sand mixture for a barrier installation. This conclusion is a generalization of the similar well known statement for simpler case of unidirectional GW flow along uniform aquifer. In this case the ratio  $K(p_{opt})/K_s$  is of large importance. An additional factor in waste depository case is  $K_w$ . Especially the large waste conductivity, i.e. condition (2.5) is unfavorable. Thus, the measurement of the hydraulic conductivity ratio  $K_s/K_w$  is an important task.

### *2.7. Method of HC Ratio Measurement*

The information about soil HC and waste depository HC is necessary as a function of depth because of HC's dependence on depth. This is a routine measurement for soil. Since the depository is toxic, these measurements are difficult and direct  $K_w$  measurement should be avoided. It is sufficient to measure convergent or divergent GW velocity distribution upstream of depository. The convergency corresponds to HC ratio smaller than 1 and the divergency corresponds to HC ratio larger than 1.

### *2.8. Possibility of HC Decline Prevention for RM/Sand Mixture at Optimal Mixing Regime*

Let us consider an RM/monodisperse sand (soil) mixture prepared in two very different mixing regimes:

- a) Regime of ideal mixing (Fig. 12a),
- b) Regime of weak mixing (Fig. 12b).

If RM particles are distributed uniformly between sand particles then it is called ideal mixing. Perhaps the ideal mixing cannot be realized so we will consider real mixing which is close to the ideal one.

In weak mixing (partially segregated), small portions of RM particles are preserved between sand particles in distinction from ideal mixing. When the difference in mean dimensions of RM and sand is three or more times, the number of RM particles exceeds the number of pores between sand particles (this number is 27 or more times larger than the sand particle numbers). If the number of RM particles exceeds the pore number and RM particles are uniformly distributed within the sand particles then all or most of the pores are filled with RM particles at almost ideal mixing.

For the ideal mixing, the deposit growth on RM particle inside a pore decreases the free space in the pore. As majority of pores are filled with RM and as HC of any pore declines due to

either chromium compound formation or Ca<sup>++</sup> salt deposition, the entire HC of RM/sand mixture decreases approximately as much as local HC decrease. This decrease in HC may be negligible in the case of weak mixing because there is only a local HC decrease inside RM particle portion. If the local HC of RM particle portion is reduced by 1000 times, it will only cause 10% decrease in the HC of RM/sand mixture. This is because the high HC of sand is preserved and the sand occupies 80-90% of RM/sand mixture space at RM  $p_{opt}$  of 0.1-0.2. In other words, there is local HC decrease inside isolated RM particle portions, which occupy 10-20% of the space of RM/sand mixture, that cannot cause the decrease of mixture entire HC, exceeding 0.1-0.2, according to reliable theory of transport phenomena in disperse systems [15] (Appendix 6). There will be retardation in the transport step of chromium reduction process in the case of weak mixing. However, this retardation can be neglected at proper weak mixing (Appendix 6). It is not easy to exclude that optimized weak mixing can prevent a large HC reduction even at  $p_{opt} > 0.2$ .

### 2.9. Layered Mixing of RM with Sand (Soil)

The perspective of  $p_{opt}$  increase at optimized weak mixing is of great technological importance. However, this optimization will be very difficult because its modeling and control are not easy. The experimental results obtained for mixing in a small volume cannot be used for the prediction of large scale mixing. The mixing results control means the determination of RMPP of their dimensions that is a time consuming process. Unfortunately, a simpler procedure of the mixing results evaluation by means of HC measurements is even more difficult than RMPP distribution characterization. This is because HC is of interest not for initial moment but after the chromium or calcium deposit formation and that takes many months. This is the advantage of RMPP determination since its measurement soon after the mixing enables us to predict the long term HC decrease. Thus, the weak mixing technology will not be more difficult than conventional technology of sand RM mixing for barrier. Moreover, the energy consumption will be decreased because weak mixing takes less time than ideal mixing. However, the investigations for optimized regime determination will be very time consuming and expensive.

A simpler approach to prevent large HC decrease at chromium reduction deserves attention. We introduce a qualitative different approach called layered mixing. Instead of mixing RM and sand, horizontal layers of RM and sand particles are formed and arranged as a periodical structure (Fig. 13). Since the high HC condition is preserved within sand layers, the decrease in HC will only take place within the RM layers. The HC of this layered system is given as:

$$K_l = \frac{d_s K_s + d_{RM} K_{RM}}{d_s + d_{RM}} > \frac{d_s}{d_s + d_{RM}} K_s \quad (2.14)$$

This equation is of large technological importance if  $K_l$  can be  $0.5 K_s$  or larger. Two advantages can be achieved with this layered structure. First, the condition (2.13) is satisfied, i.e. bypassing can be avoided. Second, the larger volume fraction of RM needed to provide the required reactive capacity of a barrier with reasonable thickness can be easily satisfied.

The property of powder to flow along narrow vertical capillary under gravitational influence can be used for producing a layered powder structure. A vertical capillary is opened from both sides. The capillary's upper opening is used for its continuous feeding with either sand or RM. The flow along capillary is accompanied with the formation of narrow vertical stream.

The deposit formation due to this stream can be controlled with the horizontal velocity of the capillary horizontal movement. The larger the velocity, the thinner will be the layer. A slit capillary can be used instead of cylindrical one. It will provide a slit like vertical powder stream. Its horizontal dimension can be as long as necessary, for example 1-3 meters. This enables us to form layer structure on a large surface (10 m<sup>2</sup> or more). By using two slit capillary, two layers namely a sand layer and an RM layer can be formed together. If sand capillary is first in the direction of capillary's horizontal movement a sand layer is formed and then an RM layer is formed over the sand layer.

A simple mechanical device for layered powder two-component system formation can be designed for its application in a trench for barrier. The growth of layered system height within the trench is accompanied with its weight increase and the system compaction. Some distortion of layered system during compaction is possible. The layers are bent or even some cracks are developed. However, a mixing process is necessary to destroy layered system completely. But there is no mixing process within the barrier so the partial distortion of layered system will not cause a serious change in its high HC. Another possibility is the industrial production of layered system as blocks and incorporation of blocks into the trench. In layered system, GW flows mainly along the sand layer and chromium ions penetrate from this flow into RM layer due to molecular diffusion. The diffusion is a slow process. The exact theory of diffusion of chromium into RM layer is under preparation. According to preliminary evaluation, the necessary layer thickness is between 5 mm and 2 cm.

### 2.10. Preliminary Evaluation of Barrier Critical Thickness

In Table 2, the values are calculated for a barrier thickness of 1 meter. A larger thickness can be used as well. The larger thickness enables us to provide larger amount of RM. On the other hand, very large thicknesses are not admissible. Thus, the concept of barrier critical thickness  $d_{bcr}$  is valuable.  $d_{bcr}$  is the minimal barrier thickness which provides reduction for 20 years. It means that 1 cm<sup>3</sup> of barrier will accumulate the maximum chromium amount. Thus  $c_{RM}$  is substituted into equation (1.2) to yield:

$$d_{bcr} = \frac{n_1 u T_b}{c_{RM}} \quad (2.15)$$

In the case of barrier installation using RM soil mixture, its capacity  $c_{mix}$  has to be substituted into equation (2.15).

$$d_{bcr} = \frac{n_1 u T}{c_{mix}} \quad (2.16)$$

where;

$$c_{mix} = p c_{RM} \quad (2.17)$$

Indeed, the larger the RM volume fraction  $p$ , the larger its surface area within 1cm<sup>3</sup> of mixture and correspondingly, the larger is the mixture reactive capacity. The specification of equation (2.16) using equation (2.17) yields:

$$d_{bcr} = \frac{u n_1 T_b}{c_{RM} p_{opt}} \cdot \frac{2K_w}{K_w + K_s} \quad (2.18)$$

where the optimal volume fraction for RM is accounted for as well. For condition (2.5), the second multiplier value approaches to 2. It means the larger HC of waste depository can cause

the necessity to increase the barrier thickness twice. The value 2 for the multiplier is a useful approximation as  $K_s$  is small as compared to  $K_w$  and can be omitted in the denominator. For condition (2.4) a large decrease in the barrier thickness is possible because almost linear decrease of GW flow rate through the barrier takes place with decreasing HC of waste depository. For the preliminary evaluation of the barrier thickness, the second multiplier in equation (2.18) is replaced with 1 because the information about the ratio  $K_w/K_s$  is not available. The influence of RM aging on the RM/soil mixture HC is still under investigation. Thus, the  $p_{opt}$  value of 0.2 recommended in the literature is substituted into equation (2.18). For the three sites, the values for chromium concentration in GW and GW velocities are taken from Table 2 and are substituted into equation (2.18). The value of  $20 \text{ mg/cm}^3$  is taken for  $c_{RM}$ .

Table 4. Predicted thickness,  $d_{bcr}$  for barriers (assuming no bypassing), meters

Barrier lifetime (years)	Allied Signal	P.P.G.	Chemical Land Holding
5	1	1	3 - 5
20	1 - 2	3 - 4	12 - 20

### 2.11. Suitability of RM Monodisperse Sand Mixture for Barrier Installation for Allied Signal and P.P.G. Using Optimal Weak Mixing Procedure or Layered RM and Sand

The barrier thickness of 1-2 m for Allied Signal is admissible. Even 3-4 m for P.P.G. is admissible but not desirable. However, the decrease of HC due to chromium accumulation or calcium deposit formation in RM sand mixture may cause complications. The use of optimal weak mixing procedure (Section 2.9) can eliminate these complications. Moreover, for P.P.G. the possibility of necessary increase in  $p_{opt}$  and correspondingly, the decrease in  $d_{bcr}$  cannot be excluded. On the other hand, if  $K_w$  for P.P.G. is far higher than  $K_s$ ,  $d_{bcr}$  increases twice according to equation (2.18). If it will be so, the possibility of  $p_{opt}$  increase due to optimal weak mixing will be important. Weak mixing procedure or layered powder system can provide two advantages:

- prevention of large HC decrease with RM addition to soil even without the application of optimal fraction of sand instead of soil and
- prevention of large HC decrease using large RM volume fraction (0.3-0.5) as the optimal sand fraction instead of soil.

The realization of both the advantages simultaneously is questionable. The choice between the two will be possible after information about  $K_s$ ,  $K_w$ ,  $K(p_{opt})$  etc. will be available.

## 3. Conditions of RM/Sand Mixture and their Suitability for Barrier Installation with Minimal Bypassing

### 3.1. Bypassing Around Barrier and Its Critical Thickness

A barrier with an invariant thickness,  $d_b$  and hydraulic conductivity,  $K_b$  is considered. The barrier has an arc shape with an angle of  $\pi/2$ . The hydrodynamic task pertaining to this problem is formulated and solved in Appendix 7 for the first crude approximation. The results are discussed here.

The GW stream entering the WD splits into 2 parts, one flowing through the barrier and the other bypassing it. The first stream is cleaned and the second stream preserves the initial

chromium concentration, namely that in aquifer. If the barrier HC is smaller than the soil HC, bypassing is not avoidable. The question arises: how much bypassing is admissible?

The bypassing is not harmful if the entire amount of chromium in bypassing flux, i.e.  $I_s n_i$  does not exceed that in GW cleaned with the barrier:

$$\frac{I_s n_i}{I n_{eff}} \leq 1 \quad (3.1)$$

where  $I$  and  $I_s$  are fluxes into WD and around the barrier, respectively.

Fresh iron-pyrite mixture can provide effluent concentration of around 0.1 ppm. In the barrier, the back layer remains fresh even as the barrier volume is contaminated 99% (Section 6). Thus for  $n_i$ , its value of 0.1 can be substituted into equation (3.1) to yield:

$$3 \cdot 10^{-3} < \frac{n_{eff}}{n_i} < 10^{-2} \quad (3.2)$$

for  $15 \text{ ppm} < n_i < 50 \text{ ppm}$  that corresponds to dissolved chromium concentration for different sites. Combining equations (3.1) and (3.2), we obtain:

$$\frac{I_s}{I} < 3 \cdot 10^{-3} - 10^{-2} \quad (3.3)$$

In Appendix 7, bypassing dependence on the parameters characterizing a barrier and a depository is obtained which is combined with condition (3.3) as:

$$\frac{I_s}{I} = \frac{K_w d_b}{(K_w + K_s)R} \left(1 - \frac{K_s}{K_b}\right) < 3 \cdot 10^{-3} - 10^{-2} \quad (3.4)$$

The equation is clear qualitatively. The thicker the barrier (larger  $d_b$ ), the smaller is its hydraulic conductivity,  $K_b$  and stronger is the bypassing. At condition (2.5), i.e. at smaller soil conductivity, equation (3.4) becomes:

$$\frac{I_s}{I} \cong - \frac{K_s}{K_b} \cdot \frac{d_b}{R} \quad (3.5)$$

Naturally, the conductivity ratio is important and not their absolute values. Two hydrodynamic resistances, namely that of waste depository (WD) and that of barrier are present in equation (3.5). Hydrodynamic resistance is directly proportional to length and inversely proportional to HC, i.e. it is  $d_b/K_b$  for a barrier and  $R/K_w$  for a depository. The sequence of a depository resistance and a barrier resistance controls the GW stream through the barrier. If a barrier resistance is negligible in comparison with that of depository, the barrier does not influence on the GW flow, i.e. the bypassing caused with barrier is negligible. The larger the barrier resistance, the larger is its influence on GW flow within depository and the larger will be the bypassing. This is expressed on the right side of equation (3.5), which is the ratio of barrier hydrodynamic resistance to that of WD.

Let us introduce the concept of critical barrier thickness,  $d_{bH}$  caused by the bypassing phenomenon.

$$d_{bH} = (3 \cdot 10^{-3} - 10^{-2})R \frac{(K_w + K_s)}{K_w} \left(\frac{K_s}{K_b} - 1\right)^{-1} \quad (3.6)$$

At a barrier thickness larger than  $d_{bH}$ , bypassing takes place. As the RM/sand mixture is used at a barrier installation,

$$K_b = K_{mix} = K_s / y \quad (3.7)$$

where;

$$y = \frac{K_s}{K_{mix}(p_{opt})} > 1$$

This case only corresponds to bypassing. The specification of equation (3.6) with the use of equation (3.7) yields:

$$d_{bH} = (3 \cdot 10^{-3} - 10^{-2})R \left( \frac{K_s + K_w}{K_w} \right) (y - 1)^{-1} \quad (3.8)$$

Table 5. Critical barrier thickness for different values of  $K_s/K_w$ ,  $R$  and  $y$

$K_s/K_w \rightarrow$ $R \text{ (m)} \downarrow$	0.3	1.0	3.0
		<b>y = 2</b>	
50	0.2 – 0.65	0.3 – 1.0	0.6 – 2.0
100	0.4 – 1.3	0.6 – 2.0	1.2 – 4.0
200	0.8 – 2.6	1.2 – 4.0	2.4 – 8.0
		<b>y = 4</b>	
50	0.07 – 0.22	0.1 – 0.33	0.2 – 0.7
100	0.13 – 0.4	0.2 – 0.7	0.4 – 1.3
200	0.23 – 0.7	0.4 – 1.3	0.8 – 2.6

### 3.2. Conditions for Remediation Using RM/Sand Mixture for Barrier Installation

Two critical thicknesses,  $d_{bH}$  and  $d_{bc}$  were introduced. A barrier thickness has to be larger than  $d_{bc}$  to provide the entire barrier capacity, i.e.

$$d > d_{bc} \quad (3.9)$$

Also, the barrier thickness has to be smaller than  $d_{bH}$  to eliminate strong bypassing, i.e.

$$d < d_{bH} \quad (3.10)$$

The information about the sites, namely its effective radius  $R$ , HC of surrounding soil,  $K_s$ , HC of waste,  $K_w$ , chromium concentration in GW stream,  $n_i$  and its velocity,  $u$  are necessary for the calculation of  $d_{bc}$  and  $d_{bH}$ . In addition, the long term investigations for the determination of RM capacity and HC for optimal RM volume fraction in mixture  $K(p_{opt})$  are necessary. The comparison of the determined values for a barrier critical thickness can lead to 2 variants:

$$d_{bH} < d_{bc} \quad (3.11)$$

and

$$d_{bH} > d_{bc} \quad (3.12)$$

If case (3.11) takes place for a site, the RM/sand mixture is not suitable for a barrier installation. Indeed  $d$  has to exceed  $d_{bc}$  according to condition (3.9). It means that  $d$  will exceed  $d_{bH}$ , according to equation (3.11). This corresponds to strong bypassing. Equation (3.12) is the condition for the possibility of remediation using RM/sand mixture for a barrier installation. Equation (3.12) allows us to choose the barrier thickness according to the rule:

$$d_{bH} > d > d_{bc} \quad (3.13)$$

If  $d$  exceeds  $d_{bc}$ , the entire critical barrier capacity will be provided. If  $d$  is less than  $d_{bH}$ , the bypassing will be either absent or sufficiently weak.

#### 4. Different Variants of Barrier Hydrological Design

##### 4.1. Advantage of Continuous Barrier Configuration and Disadvantage of Funnel and Gate System Regarding Chromium Reduction at High pH

In this investigation, a modest RM capacity at high pH is established and therefore, the continuous barrier configuration has advantage over the funnel and gate system. The critical barrier capacity was evaluated above regarding continuous configuration. As it can be seen from Table 4, a rather large barrier thickness is necessary for P.P.G. and C.L.H. to increase RM amount inside a barrier.

Regarding funnel and gate configuration, the evaluated barrier thickness within gate has to be increased  $g$  times, where  $g$  is the ratio of the gate length to the gate width. This is caused by the necessity to preserve RM amount within the barrier, i.e. to preserve entire volume of a barrier at the transition from the continuous configuration to funnel and gate configuration. Thus, if the length of RM layer decreases  $g$  times, its thickness has to be increased  $g$  times. Also, the velocity through the gate has to be  $g$  times larger. This is possible with the increasing HC within the gate. Meanwhile, RM and even RM/soil mixture usually have smaller HC. Thus, the problem of providing a large capacity and high HC at the same time becomes more difficult with the use of funnel and gate configuration.

The advantage of a funnel and gate system over an in-situ reaction curtain is that a smaller reactive barrier can be used for treating a given plume that may lead to lower cost. If the barrier requires periodic replacement, it will be easier to accomplish if this barrier is enclosed in a relatively small gate than if it is spread across a large extent of aquifer, as in the case of in-situ reaction curtain [16]. As a rather large amount of RM is necessary to accumulate chromium, the reactive barrier enclosed in a relatively small gate becomes impossible. This is even more difficult as RM has to be mixed with a large amount of soil or sand (5-10 times).

##### 4.2. Variable Thickness of Barrier in the Continuous Configuration

In the absence of a barrier, the radial velocity changes very strongly along the back boundary of waste depository with its maximum value at back pole and its zero value near the equator. This distribution is preserved with a barrier installation because the bypassing has to be avoided. This means the contaminated GW stream through barrier changes along its length. Correspondingly, the amount of chromium accumulated within the barrier is maximum near the back pole of depository and decreases as it approaches the equator. As the barrier thickness has to be proportional to the chromium flux through it and the latter changes along it, the variable thickness of barrier is reasonable (Fig. 14). As the maximum barrier thickness necessary in the vicinity of its back pole is very large, a decrease in installation expenses can be achieved by decreasing the barrier thickness as it approaches the equator.

### 4.3. Barrier Configuration Supplemented with Upstream Cutoff Walls

According to Table 4, a very large barrier thickness will be required in the case of C.L.H. and the use of in-situ reaction curtain would be impracticable. In this situation the idea formulated in [16] deserves an attention: "A contaminant source zone can be completely surrounded by cutoff walls except for a gap that is left on the down gradient side. The upstream wall deflects most of the groundwater around the contaminant source zone. Water that infiltrates into the enclosure or flows through the cutoff walls into the cell exits through the gap, where an in-situ reactor remediates the groundwater. This configuration minimizes the amount of water that flows through the contaminant source zone and hence the amount of contaminated ground water that must be treated. It also maximizes the retention time in the gate which leads to more complete treatment [16]" (Fig. 15).

### 5. Reactive Filter (PRB with Channels)

In spite of all the advantages, a serious shortcoming is inherent to conventional PRB technology. It cannot provide simultaneously a large reactive capacity and high HC. Although, the optimal weak mixing and layered RM/sand structure (Section 2) can improve the situation but this approach is not sufficient for the Chemical Land Holding case. A sufficient reactive capacity can be provided with the critical barrier thickness of 3-4 m if the trench will be filled with RM at volume fraction of 0.9. It is questionable that layered RM/sand structure can work with so large  $p_{RM}$ .

A qualitative different hydrodynamics for PRB realization is proposed that enables higher HC for PRB, even 1000 times (Appendix 8) at  $p_{RM} = 0.9$  or larger. The decrease of RM layer thickness causes a decrease in barrier HC. At the same time, barrier capacity decreases which is not acceptable. Both high HC and high capacity of barrier can be provided by means of extending filtration area. If filtration area decreases  $n$  times, the flow rate density decreases  $n$  times (at the same entire flow rate). It means the pressure drop decreases  $n$  times because it is proportional to flow rate density. The necessary increase of the filtration area and the corresponding decrease of hydrodynamic resistance can be provided by the incorporation of transport channels in PRB (Fig. 16). As water transport is provided by its movement along the ensemble of thin channels crossing the barrier in the direction of GW stream, the free space between channels can be filled with RM only, i.e. there will be no necessity of RM mixing with soil or other inert filler.

It is possible to increase RM volume fraction within PRB to 90% because 10% of space will be occupied with transport channels. Thus, the new type of PRB will provide a possibility of remediation even under strong RM passivation because the strong decrease in RM capacity caused by passivation will be compensated with the increase of RM volume fraction (correspondingly RM surface area) within the barrier. In other words, RM capacity decrease will not cause a decrease in PRB capacity. This technology enables us to create PRB with large reactive capacity and simultaneously at admissible barrier thickness, in particular  $C_{bcr} = 100$  mg/cm<sup>3</sup> and  $d_{bcr} = 4$ m which solves the problem of C.L.H. plume remediation. The incorporation of transport channels into PRB makes its HC larger than soil HC, even if the latter is large. It creates an opportunity to decrease the barrier length and therefore, the expenses.

## 6. Nearly Uniform or Nonuniform Chromium Accumulation Within Barrier and Its Critical Thickness: Dynamics of Chromium Distribution within Barrier

The notion of critical barrier capacity which enabled us to introduce barrier critical thickness and therefore to model long-term performance of a barrier (Sections 1.4 & 1.5) uses the assumption of uniform chromium distribution within a barrier. This assumption enables us to introduce the specific barrier capacity as:

$$c_{bcr} = C_{bcr} / d_b \quad (6.1)$$

where  $C_{bcr}$  is the entire critical capacity of barrier. For nonuniform chromium distribution across a barrier the density of accumulated chromium is an unknown function of the distance to the barrier front surface. The notion of  $c_{bcr}$  according to equation (1.2) and the main condition (1.3) become useless. Correspondingly, the prediction of critical barrier thickness according to equation (2.16) becomes useless too.

There are no publications devoted to dynamics of chromium accumulation within the barrier. Even the assumption about uniform distribution that enabled us to calculate barrier critical thickness is not introduced in the literature. The PRB dynamic model has to be elaborated using the conservation equation for chromium and the equation for reduction kinetics. These two equations enable us to calculate two non-steady distributions, one for accumulated chromium,  $\rho(x,t)$  and the other for dissolved chromium,  $n(x,t)$ , where  $x$  is the distance to the barrier front surface (Fig. 17). The dynamic model in combination with accomplished measurement of chromium reduction kinetics (Section 1) confirms the assumption about uniform chromium distribution as a first approximation. The dynamics introduces an essential correction to this assumption. It is not valid for the whole barrier. It is valid for one of its three parts (Fig. 17).

The results of joint solution for two equations aforesaid can be formulated as a 3 layer dynamic model for the accumulated chromium distribution. The layer numeration corresponds to the direction of GW flow through a barrier. The chromium accumulated during the barrier life is located near the barrier front surface. This first layer can be called accumulation layer. The third layer adjacent to a barrier back surface almost does not contain any chromium. The second layer (located between first and third ones) can be called reduction layer because the reduction takes place within it. Indeed, there is no reduction within the first layer because it starts after the accumulation of maximum possible amount,  $C_{RM}$  in any  $\text{cm}^3$ . Also, there is no reduction in the third layer because it is reduced in the second layer.

The uniform distribution of chromium within layer 1 happens because the reduction stops at same accumulated chromium density  $\rho(x) = c_{RM}$  for any  $x < x_a(t)$ , where  $x_a(t)$  is the current thickness of accumulated layer. As there is no reduction within the accumulated layer, the dissolved chromium concentration does not change as GW flows through this layer, i.e. its concentration equals to initial one within the layer.

$$n(x,t) = n_i \quad x < x_a(t) \quad (6.2)$$

$n(x,t)$  decreases rapidly as GW flows through the second layer because of its reduction and accumulation.  $n(x,t)$  approaches to the effluent concentration within third zone.

$$n_e < n(x,t) < n_i \quad \{x < x_r(t)\} \quad (6.3)$$

$$n(x,t) \sim n_e \quad \{x_r(t) < x < d_b\} \quad (6.4)$$

where  $x_r(t)$  is the boundary between second and third layers. The shape and thickness of the second layer do not change with time. Its thickness is small in comparison with  $d_b$  and the entire amount of chromium accumulated within a barrier can be identified with the accumulation in the first layer.

$$n_i u t = c_{RM} x_a(t) \quad (6.5)$$

$$x_a(t) = \frac{n_i u t}{c_{RM}} < d_b \quad (6.6)$$

The effluent concentration starts to increase as third layer disappears. Since the thickness of second layer is small, therefore:

$$x_a(t) = \frac{n_i u T_b}{c_{RM}} \sim d_b \quad (6.7)$$

This justifies equation (2.15) for critical barrier thickness.

## References

1. Powell, R. M., Puls, R.W., Hightower, S. K. and Sabatini, D. D., *Environ. Sci. Technol.*, 29, (1995), 1913-1922.
2. Powell, R. M., Puls, R.W. and Paul, C. J., "Innovative Solutions for Contaminated Site Management," *Ware Environment Federation*, Miami, FL, 1994, 485-496.
3. Stollenwerk, K. G. and Grove, D.B., *J. Environ. Qual.*, 4, (1985), 396-399.
4. Blowes, D. W., Ptacek, C. J. and Jambor, J. L., *Environ. Sci. Technol.*, 31, 12, (1997), 3348-3357.
5. Eary, L. E. and Rai, D., *Environ. Sci. Technol.*, 22, (1988), 972-977.
6. Saleh, F. Y., Parkerton, T. F., Lewis, R.V. Huang, J. H. and Dickson, K. L., *Sci. Total Environ.*, 86, (1989), 25-41.
7. Palmer, C. D. and Wittbrodt, P. R., *Environ. Health Perspect.*, 92, (1991), 25-40.
8. Nriagu, J., Beaubien, S. and Blowes, D. W., *Environ. Rev. 1*, (1993), 104-120.
9. Eary, L. E. and Rai, D., *Am. J. Sci.*, 289, (1989), 180-213.
10. Anderson, L. D., Kent, D. B. and Davis, J. A., *Environ. Sci. Technol.*, 28, (1994), 178-185.
11. Kriegman-King, M. R. and Reinhard, M., *Environ. Sci. Technol.*, 28, (1994), 692-700.
12. Anderson, L. D., Kent, D. B., Davis, J. A., *Environ. Sci. Technol.* 28, (1994), 178-185.
13. McMahon, P. B., Dennehy, K. F. and Sandstrom, M. W., *Ground Water*, 27, (1999), 395-404.
14. O'Hannesin, S. F. and Gillham, R.W., *Gr. Water Monit. Remed. 1*, (1998), 164-170.
15. Dukhin, S. S. and Shilov, V. N., *Dielectric Phenomena and the Double Layer in Disperse Systems and Polyelectrolytes*, John Wiley, New York, 1974, Chapter 2, paragraph 1 (Dielectric Phenomena in a Mixture of Components with Different Conductivities) and Chapter 6, paragraph 2 (Principle of Generalized Conductivities).
16. Starr, R. C. and Cherry, J. A., *Ground Water*, 12(3), (1994), 465-476.
17. Ijoor, G. C., "Modeling of a Permeable Reactive Barrier," *Masters Thesis*, New Jersey Institute of Technology, Newark, NJ, 1999.

**APPENDICES**

**Appendix 1**  
**Information About Iron 2 and Iron 3**

Table A.1.1. Particle sizes of iron 2 and iron 3

Iron 2		Iron 3	
Sieve size	Percentage retained	Sieve size	Percentage retained
50	0	60	0.0
60	2	80	0.6
70	20	100	4.0
80	17	325	73.2
100	25	Pan	22.0
120	11		
Pan	25		

**Appendix 2**  
**Solubility of Pyrite and Siderite**

The most important examination concerning the pyrite and siderite relates to their solubilities. It is possible that they dissolve in less than 20 years that will make the barrier useless. The handbook data for the solubility of pyrite and siderite is given as:

Pyrite: 0.0005 gr/100 cm<sup>3</sup> (or 1 gr/2 x 10<sup>5</sup> cm<sup>3</sup>)

Siderite: 0.007 gr/cm<sup>3</sup>

For the complete dissolution of 1 gram of pyrite, the critical volume of water is necessary which is given as:

$$v_{cr} = 2 \times 10^5 \text{ (cm}^3\text{/gr)} \quad (\text{A.1.1})$$

Let us consider a barrier cross-section perpendicular to groundwater stream with area,  $S$  and the pyrite volume in barrier,  $Sdp_p$ , where  $d$  is the barrier width and  $p_p$  is pyrite volume fraction. During time,  $T_b$ , the groundwater volume,  $uT_bS$  crosses this cross-section of the barrier, i.e. this volume is available to dissolve the pyrite volume with the mass  $Sd\rho p_p$  where  $\rho$  is the pyrite density. Thus the ratio:

$$v_b = \frac{uT_bS}{d\rho S p_p} = \frac{uT_b}{d\rho p_p} \cdot \left( \frac{\text{cm}^3}{\text{gr}} \right) \quad (\text{A.1.2})$$

where  $u$  (cm/day) and  $T_b$  (day) has to be compared with  $v_{cr}$ . With  $d=100$  cm and  $T_b = 20$  years, the results are given in Table A.2.1

Table A.2.1. Groundwater volume per gram of RM in a barrier for its 20 years work

$p_p \rightarrow$	0.5	1.0
$u$ (cm/day) ↓		
100	$3 \times 10^4$	$1.5 \times 10^5$
10	$3 \times 10^3$	$1.5 \times 10^4$

Small pyrite volume fraction corresponds to the RM soil mixture with RM volume fraction 0.2. It can be seen that the pyrite solubility within barrier in this case is not negligible.

Nevertheless, this complication may not arise because GW velocity is much smaller (Table 2). Siderite solubility is 5 times larger. Siderite application in mixture with soil at large GW velocity is not reasonable.

### Appendix 3

#### *A.3.1. Importance of Individual Investigations of Passivation Kinetics and Hydraulic Conductivity Decline Regarding Individual Characteristics of Every Site*

The reduction of passivation and corrosion is very difficult to quantify. One concludes that RMC dependence on flow rate and influent concentration needs to be investigated with experiment. With account for long term character of these experiments the parallel investigations with different pair values (velocity, concentration) are necessary. Even with 10 parallel experiments a rather small number of combinations of values for velocity and influent concentration is possible. The velocities and concentrations for the three sites vary in rather wide range. Since the function describing the RMC dependence on velocity and concentration will not be exact, the more reliable approach is the individual modeling with account for the individual characteristic of a given site. Even with this approach, a lot of parallel measurements are necessary. Even with a single value of groundwater concentration, the large seasonal variation in velocity creates the necessity of parallel experiments with at least 3 values for velocity, namely: minimum, maximum and medium. In addition, the experiments with concentrations smaller than that of site groundwater are desirable because any layer inside the barrier is initially filled with groundwater with decreased effluent concentration produced with upstream layers. Thus the procedure of the RM suitability for a definite site consists of 2 stages:

1. The preliminary evaluation based on the RMC dependence on concentration and velocity. The error of this preliminary evaluation can be very large with account for many difficulties discussed above.
2. The more exact final evaluation based on the individual modeling with account for a site individual characteristics.

#### *A.3.2. Complications in Reactive Barrier Modeling Caused by Seasonal Variation in Groundwater Velocity*

Is there a correlation between chromium concentration and seasonal variation of groundwater velocity? The seasonal variation in groundwater velocity is large and correspondingly the large variation can arise in the prediction of critical barrier capacity if the maximum or the minimum velocity will be substituted in equation (1.2). Neither the minimum nor the maximum velocity has to be used in this prediction. According to the general definition of RBC, it is the total amount of chromium in groundwater stream crossing the barrier during 1 year divided by the barrier length and multiplied by the entire duration of barrier life,  $T_b$ . If the velocity changes and can be represented as function of time, equation (1.2) has to be generalized:

$$\frac{n_i}{d_b} \int_0^{year} u_b(t) dt \sim \frac{n_i}{d_b} \sum u_{bk} \Delta t_k \quad (A.3.1)$$

and

$$\sum_{k=1}^m \Delta t_k = 1 \text{ year} \quad (\text{A.3.1a})$$

Since, the velocity as a function of time is measured some times per year, it can be characterized with this different discrete value. This value has to be related to the time intervals between measurements,  $\Delta t_k$ . If the maximum and the minimum velocities are known then there are only 2 time intervals. But the maximum and minimum velocities cannot be found without many measurements with small time intervals between them. With this very poor information about groundwater stream, the situation can be evaluated as there is an equal time for the maximum and the minimum velocity. This leads to a simple result with a large error.

$$C_b = \frac{n_b}{d_b} \frac{u_{\min} + u_{\max}}{2} T_b \quad (\text{A.3.2})$$

Naturally, more information about seasonal variation for groundwater velocity is necessary. It may happen that the seasonal variations in velocity cause seasonal variations in concentration. The rainwater mixing with chromium contaminated water leads to chromium dilution and chromium concentration decrease. The mixing is possible even as rainwater layer forms due infiltration above the contaminated layer. The mixing occurs as both layers slowly move in the horizontal direction due to the head gradient. The mixing occurs as small stream envelopes a soil particle or an agglomerate and splits into 2 streams. This mixing occurs on the boundary between 2 large streams, namely: groundwater stream and fresh rainwater stream. As a result, the boundary between these layers becomes wider with the decreased chromium concentration.

#### Appendix 4

#### **Weak Bypassing Mechanism. Qualitative and Semi-quantitative Considerations (Numerical Calculations)**

A continuous barrier cross-section and a profile for hydraulic head are shown in Fig.14. As there is no difference in barrier and aquifer conductivities, the hydraulic gradient (HG) inside the barrier is identical with the regional hydraulic gradient (line 1). As the barrier conductivity is smaller than that of aquifer:

$$K_b < K_a \quad (\text{A.4.1})$$

the HG inside the barrier has to be increased to provide the GW flux through the barrier approximately the same as at large distance before the barrier. This occurs in the most interesting case of weak bypassing; that means that the GW is mainly flowing through the barrier, i.e. the barrier installation causes a weak change in hydraulic field only.

The mechanism of the HG increase inside the barrier is clear. As GW meets larger hydrodynamic resistance entering the barrier, the head grows up before the barrier (curve 2). Correspondingly, head decreases behind the barrier. This head increase (decrease) is an unknown function of distance to the barrier surface,  $h_l(z)$ . Naturally, it decreases with the increasing distance to the barrier because at rather large distance, the regional gradient realizes. The dependence of  $z$  on  $h_l$  is shown qualitatively in Fig. 18.

The additional head changes along the barrier as well, i.e. it is a function of coordinate  $x$ ,  $h_1(z,x)$ . As the barrier length is  $L$ , we nominate  $x = 0$  in the barrier center and correspondingly  $x = L/2$  at the barrier's edge. The additional head arises due to the presence of a barrier. It means it is negligible far from barrier in  $x$  direction as well. It does not mean that the additional head  $h_1$  is absent near the barrier edge. But it is smaller there, i.e.  $h_1$  is the function with its maximum at  $x = 0$  and monotonous decrease with the increasing  $x$ . This HG decrease along the barrier causes GW flow from the barrier center to its edges,  $x = \pm L/2$ . This tangential (regarding the barrier) flow is the first step of bypassing. This flow behind the barrier edges bypasses it. This simplified picture enables us to evaluate the bypassing dependence on the barrier thickness,  $d_b$  and length. The tangential HG can be evaluated as a ratio,  $h_1(z,0)/(L/2)$ , the normal gradient as  $2h_1(0,x)/d_b \sim 2h_1(0,0)/d_b$ . Now the entire normal flow can be evaluated as:

$$I = K_b \frac{2h_1(0,0)}{d_b} L \quad (\text{A.4.2})$$

and the entire tangential flow as:

$$I_s = \frac{2K_a h_1(0,0)}{L} \varepsilon \cdot L \quad (\text{A.4.3})$$

where  $\varepsilon$  is an unknown multiplier. The calculation of the entire tangential flow needs information about  $z$  dependence for  $h_1(z,x)$ . Since, the latter is absent we assume that  $h_1$  is non-zero within distance  $L$  from the barrier and correspondingly, the tangential flow extends over this distance. It means that the entire tangential flow is proportional to  $L$ . However, the larger the value of  $z$ , the smaller the value of  $h_1$  and its tangential derivative, i.e. the tangential flux density is evaluated with the use of  $h_1(0,0)$  instead of  $h_1(z,0)$ . It means that the coefficient  $\varepsilon$  introduced in equation (A.4.3) for the correction is smaller than 1. The bypassing can be evaluated as a ratio of the total tangential flow to the total flow through the barrier, i.e.

$$\frac{I_s}{I} \sim \varepsilon \frac{d_b}{L} \cdot \frac{K_a}{K_b} \quad (\text{A.4.4})$$

Note, that this evaluation does not comprise the case of extremely weak bypassing, namely the case of small difference between barrier and aquifer conductivities. In this case the normal flux is proportional to the regional gradient because  $h_1$  is extremely small. We neglected this term assuming that  $h_1$  is not very small that caused the cancellation of unknown  $h_1(0,0)$  at the ratio (A.4.4) evaluation. To provide this cancellation, the case  $(K_a - K_b) \ll K_a$  was excluded. The numerical calculations confirmed this quantitative picture [17]. The bypassing is characterized with GW trajectories obtained with numerical calculation (Fig. 19). The contaminant loss increases with increasing barrier thickness as illustrated in Fig. 20. The contaminant loss decrease with increasing barrier length is illustrated in Fig. 21.

## Appendix 5 Streamlining Around Circular Waste Depository

A set of simplification is used to make the analytical solution easier. A flat horizontal surface of aquitard and isotopic aquifer HC uniform in space are assumed. At this condition the hydrodynamic velocity does not depend on the elevation head,  $Z$ , and the GW flow field can be

described by two dimensions. The steady state conditions for GW are assumed. Correspondingly, the steady state Laplace equation for hydraulic head can be used:

$$\frac{\partial^2 h}{\partial r^2} + \frac{1}{r} \cdot \frac{\partial h}{\partial r} + \frac{1}{r^2} \cdot \frac{\partial^2 h}{\partial \theta^2} = 0 \quad (\text{A.5.1})$$

where the cylindrical system of coordinate is characterized in Fig. 10.

Equation (A.5.1) has to be considered inside and outside of the depository where the hydraulic conductivities are different. Thus, the hydraulic head distribution inside a depository,  $h_w(r, \theta)$  and outside of it  $h_s(r, \theta)$  have to be introduced. Both distributions satisfy Laplace equation (A.5.1). Its solution can be obtained by the method of independent variable separation, namely in the form:

$$h(r, \theta) = R(r)\Theta(\theta) \quad (\text{A.5.2})$$

This substitution of this expression into equation (A.5.1) yields ordinary differential equations for functions  $R$  and  $\Theta$ .

$$r \frac{d}{dr} \left( r \frac{dR}{dr} \right) - n^2 R = 0 \quad (\text{A.5.3})$$

$$\frac{d^2 \Theta}{d\theta^2} + n^2 \Theta = 0 \quad (\text{A.5.4})$$

Their solutions are  $R_n(r)$  and  $\cos n\theta$ ,  $\sin n\theta$ , where  $n = 1, 2, \dots$ . At large distance from depository upstream, the hydraulic gradient distribution is determined by the regional hydraulic gradient value,  $V_s$ , i.e.

$$h(r, \theta) = V_s r \cos \theta \quad (\text{A.5.5})$$

This enables us to satisfy the conditions on the boundary between soil and depository i.e.  $r = R$ :

$$h_s(R, \theta) = h_w(R, \theta) \quad (\text{A.5.6})$$

$$K_s \frac{dh}{dr}(R, \theta) = K_w \frac{dh_w}{dr}(R, \theta) \quad (\text{A.5.7})$$

using the solutions of the form:

$$h_s(r, \theta) = R_{1s}(r) \cos \theta, h_w(r, \theta) = R_{1w}(r) \cos \theta \quad (\text{A.5.8}), (\text{A.5.9})$$

and to specify equation (A.5.3) with  $n = 1$ . The hydraulic head and GW flow density have to be continuous at the crossing of the boundary between soil and aquifer, i.e. at  $r = R$ . These conditions are expressed with equations (A.5.6) and (A.5.7). Since,

$$R_{1s} = \frac{1}{r}, R_{1w} = r \quad (\text{A.5.10})$$

the solutions have to be sought as:

$$h_s = V_s \left[ r + \frac{R^2}{r} (1+x) \right] \cos \theta \quad (\text{A.5.11})$$

$$h_w = V_w \cos \theta \quad (\text{A.5.12})$$

The substitution of these functions into the boundary conditions (A.5.6) and (A.5.7) transform them into linear algebraic equation for 2 unknowns,  $V_w$  and  $x$ . The solution of this system is:

$$x = -\frac{2K_w}{K_s + K_w} \quad (\text{A.5.13})$$

$$V_w = \frac{2K_s}{K_w + K_s} V_s \quad (\text{A.5.14})$$

With  $K_w = K_s$ , the solutions (A.5.11) and (A.5.12) have to be reduced to unidirectional distribution (A.5.5). This qualitative consideration is confirmed by the substitution,  $x = -1$ , that follows from equation (A.5.13) into equation (A.5.11). At this substitution, equation (A.5.11) reduces to equation (A.5.5). At equal hydraulic conductivities  $V_w = V_s$ , according to equation (A.5.14), that transforms the distribution (A.5.12) into (A.5.5) as well, the GW flux into (out) a depository has to be absent if its HC is equal to zero ( $K_w = 0$ ). This leads to  $x = 0$ , according to equation (A.5.13) and this in turn leads to zero value for  $dh_s/dr(R)$ , according to equation (A.5.11), i.e. to zero flux within the depository. The total stream of GW into depository is obtained by means of integration over its boundary in the range,  $0 < \theta < \pi/2$ :

$$Q = \int_0^{\pi/2} 2\pi R^2 K_s \frac{\partial \cdot h_s}{d \cdot r} \sin \theta d\theta = 2\pi R^2 K_s V_s x \int_0^{\pi/2} \cos \theta \sin \theta d\theta = \pi R^2 u_s \frac{2K_w}{K_w + K_s} \quad (\text{A.5.15})$$

### Appendix 6

#### **Evaluation of Small Decrease in HC and in Transport Step Rate of Chromium Reduction at Optimal Weak Mixing of RM and Sand**

To evaluate this small decrease, let us introduce a mean radius for RM particle portion (RMPP), i.e. let us neglect their distribution regarding the dimension and the deviation of their shapes from spherical one. As the HC inside RMPP decreases very much we can neglect it, i.e. HC for RMPP equals to zero. Thus, the formulation of task is that there was an initial HC of RM/sand mixture,  $K_{mix}(p_{opt})$  and afterwards RMPP becomes impermeable due to either chromium reduction or due to Ca deposit formation. Thus, there is a disperse system with impermeable spherical inclusions and their volume fraction is  $p_{opt}$  and the equation for its HC as a function of  $p_{opt}$  is necessary.

The analogy between hydrodynamics of porous media and dielectric properties of disperse system [15] can be used that enables us to apply the well known Maxwell equation:

$$\delta\varepsilon = \bar{\varepsilon} - \varepsilon_o = \frac{3\varepsilon_o(\varepsilon_1 - \varepsilon_o)}{2\varepsilon_o + \varepsilon} p \quad (\text{A.6.1})$$

where  $\varepsilon_o$  and  $\varepsilon_1$  are the dielectric permittivities of media and particles, respectively,  $\bar{\varepsilon}$  is the mean dielectric permittivity of mixture and  $\delta\varepsilon$  is the decrease of dielectric permittivity caused with particle presence. In our case HC is an analog of the dielectric permittivity. Correspondingly, an analog of equation (A.6.1) is:

$$\delta K = K_{mix}(p_{opt}) - K_s = \frac{3K_s(K_{RMPP} - K_s)}{2K_s + K_{RMPP}} p_{opt} \quad (\text{A.6.2})$$

where  $K_{mix}(p_{opt})$  is HC of RMPP/sand mixture after HC of RMPP is decreased due to the formation of either chromium deposit or calcium oxide deposit. As small HC of RMPP can be

neglected, we obtain:

$$\delta K / K_s = -\frac{3}{2} p_{opt} \quad (\text{A.6.3})$$

The HC decrease is not large even at  $p_{opt} = 0.2$ , namely 0.3.

The so-called, “principle of generalized conductivity” is used and extended above over HC of porous media. It is described in Chapter 6, paragraph 2 of reference [15]. The principle comprises of electrostatics, electrodynamics, magnetostatics, thermal conductivity and diffusion. This series is supplemented now with HC. Each among different fluxes,  $j$  satisfies the continuity equation:

$$\text{div } \vec{j} = 0 \quad (\text{A.6.4})$$

and is a linear function of the corresponding vector field,  $\vec{x}$ :

$$\vec{j} = \Lambda \vec{x} \quad (\text{A.6.5})$$

where  $\Lambda$  are phenomenological or kinetic coefficients. In our case  $j$  is GW velocity,  $x$  is hydraulic head,  $\Lambda$  is HC, and equation (A.6.6) is Darcy law. For any nature of conductivity process, the boundary conditions are the equality of the normal components of fluxes on both sides of the interfaces, i.e.

$$j_{1n} = j_{on}, \text{ i.e. } \Lambda_1 x_{1n} = \Lambda_o x_{on} \quad (\text{A.6.7})$$

and equality of thermodynamic forces:

$$x_1 = x_o \quad (\text{A.6.8})$$

These boundary conditions are similar to our boundary conditions (A.5.6) and (A.5.7). The mathematical formulation of the principle of generalized conductivity is:

$$\frac{\bar{\Lambda}}{\Lambda_o} = F\left(p, \frac{\Lambda_o}{\Lambda_1}\right) \quad (\text{A.6.9})$$

where  $\Lambda_0$  and  $\Lambda_1$  are media and particles conductivities and  $\bar{\Lambda}$  is the disperse system conductivity. For small volume fraction and for dielectric permittivity, the general equation (A.6.9) is specified as Maxwell equation (A.6.1). This enables us to apply an analog of Maxwell equation to HC, i.e. to write equation (A.6.2).

The chromium reduction is a two-step process. The first step is chromium transport from local stream of GW on a RM particle surface. The second step is chromium ion reduction on this surface. At RM/sand mixture preparation with a weak mixing, the transport step becomes slower than in ideal mixture. However, it can be sufficiently rapid at proper weak mixing. The transport step becomes slower because when the mean path for chromium transport to RM particle surface is larger, the mixing is weaker.

For evaluating the role of transport rate, the comparison of 2 characteristic times is necessary, namely the GW residence time,  $t_{res}$  within a barrier and the mean time necessary for chromium ion transport to the RMPP surface,  $t_{dif}$ . This transport occurs due to molecular (ion) diffusion that is marked with index “dif”.

By introducing a notion of mean diffusion path,  $b_D$ , the diffusion transport time can be

evaluated by using the well-known equation of Albert Einstein:

$$t_{dif} = \frac{b_D^2}{D} \quad (\text{A.6.10})$$

where  $D$  is chromium ion diffusivity. For a crude evaluation of  $b$ , let us consider a simplified model for the result of weak mixing. A mean linear dimension,  $a$  for RMPP dimension is introduced, i.e. the real distribution of RMPP dimension is neglected.

A mean distance between single RMPP is introduced, i.e. the distribution regarding this distance is neglected. Afterwards the well-known cell model is applied, namely a spherical cell with a radius  $b$  is considered with RMPP in its center. The mixture as a whole is considered as a structure consisting of these elementary cells. It means that RM volume fraction in cells equals to RM volume fraction for a mixture as a whole, i.e.

$$\frac{a^3}{b^3} = P_{opt} \quad (\text{A.6.11})$$

or

$$b = ap_{opt}^{-3}$$

and

$$(b - a) = a(p_{opt}^{-3} - 1) \sim a \quad (\text{A.6.12})$$

The application of a cell model to replace the consideration of real transport processes with its description for one cell. The maximal diffusion path within a cell equals to  $b-a$ , i.e. the mean diffusion path is smaller. Nevertheless, the maximal diffusion path will be used that leads to an over evaluation of the mean diffusion time. Now with the substitution of  $a$  instead of  $b_D$  into equation (A.6.10), we obtain:

$$t_{dif} \sim \frac{a^2}{D} \quad (\text{A.6.13})$$

With ion diffusivity of  $10^{-5}$  cm/sec,  $t_{dif}$  equals to  $10^3$  sec for  $a \sim 1$  mm. Meanwhile, the residence time for a barrier is  $10^5$ - $10^6$  sec. Thus, the residence time exceeds the time necessary for diffusion by 100-1000 times. The GW stream may enhance the diffusion transport. However, this increase is not essential because Pecklet number almost equals to 1.

$$Pe = \frac{au}{D} \sim \frac{0.1 \cdot 10^{-4}}{10^{-5}} \sim 1 \quad (\text{A.6.14})$$

This evaluation is crude, because the diffusion time has to be compared with GW residence time in one cell, which is 1000 times smaller than the residence time for a barrier. However, the chromium is consumed at GW transport through a series consisting of 1000 cells. This thousand compensates the preceding thousand. Naturally, this is a crude evaluation, as the chromium accumulation during GW stream through 1000 cells is replaced with one cell consideration only. However, the result is reliable because the residence time for a barrier exceeds the diffusion time 1000 times. A more exact quantification is possible using the theory of diffusion in bi-porous media.

As the real picture contains the elements of Figs. 12a and 12b, the notion of mean quantity of particles for RMPP,  $N$  has to be introduced. It means that RMPP number is  $N$  times

smaller than the total number of primary particles. If at ideal mixing almost all pores between sand particles are filled with RM particles, the preservation of their RMPP during weak mixing means that the percentage of pores filled with RMPP will be  $N$  times smaller at ideal mixing. The value  $N = 3-5$  is sufficient to prevent large decrease in hydraulic conductivity.  $N = 3-5$  means that 1 pore among 3-5 pores is filled with RMPP, i.e. there is 2-4 free pores in the vicinity of almost any free pores and only one adjacent pore is clogged. As other adjacent pores are free, the local water stream will change its direction, i.e. the bypassing is possible. This repetition of bypassing many times along a water streamline will cause a decrease in HC. The smaller the HC, the larger is the number,  $N$  (smaller RMPP concentration).

### Appendix 7 Bypassing of Arc Like Barrier

If a barrier is installed as an arc along the depository boundary downstream, a new boundary condition along this boundary arises:

$$K_s \frac{\partial \cdot h_s}{\partial \cdot r}(R) = K_b \frac{h_s(R) - h_s(R + d_b)}{d_b} \quad (\text{A.7.1})$$

We assume that the barrier is sufficiently thin, i.e.

$$d_b \ll R \quad (\text{A.7.2})$$

that yields the representation for hydraulic gradient inside a barrier as right side of equation (A.7.1). It means that the flux from the depository into the barrier (left side of equation A.7.1) is equal to the flux across the barrier (right side of equation A.7.1). The special case is of interest, corresponding to weak bypassing. This restriction enables the application of the method of sequent approximation. The solution is sought as the superposition of zero approximation and the first approximation,  $h_1$ :

$$h = h_0 + h_1(r, \theta) \quad (\text{A.7.3})$$

$$h_1 \ll h_0 \quad (\text{A.7.4})$$

where  $h_0$  describes the distribution before a barrier installation, i.e.  $h_0$  is characterized by equation (A.5.11)

$$h_{os} = V_s \left[ r + \frac{R^2}{r} (1 + x) \right] \cos \theta \quad (\text{A.7.5})$$

and

$$h_{s1} = V_{s1} \frac{R^2}{r} \cos \theta \quad (\text{A.7.6})$$

This substitution into equation (A.7.1) yields:

$$V_s K_s x = \frac{K_b}{d_b} (V_s x d_b + 2V_{s1} R) \quad (\text{A.7.7})$$

The first term in bracket is:

$$h_{os}(R + d_b) - h_o(R)$$

and the second term is:

$$h_{s1}(R + d_b) - h_{w1}(R)$$

It is clarified from Fig. 18 that a barrier installation causes a hydraulic head increase before the barrier and its decrease after the barrier and their absolute values are equal. Equation (A.7.6) relates to  $r > (R + d_b)$ . It means, that:

$$h_{w1}(R, \theta) = -V_{s1}R \cos \theta \quad (\text{A.7.8})$$

and correspondingly,

$$h_{s1}(R + d_b, \theta) - h_{w1}(R, \theta) = 2V_{s1}R \cos \theta \quad (\text{A.7.9})$$

Substituting into equation A.7.7, we obtain:

$$\frac{V_{s1}}{V_s} = \frac{d_b}{R} \cdot \frac{K_w}{K_s + K_w} \left(1 - \frac{K_s}{K_b}\right) \quad (\text{A.7.10})$$

As barrier and soil conductivities are equal, a barrier installation does not change hydrodynamic field, i.e. the term,  $h_{s1}$  has to be absent, that is confirmed with equation (A.7.10). At  $K_b < K_s$  and  $K_b > K_s$ , the GW stream through the barrier is larger and smaller than before its installation; that is confirmed with equation (A.7.10). As the waste conductivity is zero, there is no GW flow inside it and consequently through the barrier. As there is no flux through the barrier the distribution,  $h_{s1}$  does not arise, that is confirmed with equation (A.7.10).

The distributions (A.7.5) and (A.7.6) are identical at  $r = R$  with a difference in  $V_s$  and  $V$  values. Their substitution into equation (A.5.15) yields the entire flux of GW through the aquatory. At barrier conductivity larger than that of soil this flux decreases and this decrease is equal to the entire bypassing flow. Thus equation (A.7.10) yields the ratio of the entire bypassing flow to the entire flow. This ratio is called contaminant loss ratio because the contaminant in bypassing flow does not cross barrier and is lost for the barrier remediation. Equation (A.7.10) is a first crude approximation and has to be perfected with account for the boundary condition along the depository boundary upstream. The solution has to be a superposition of term, proportional to  $\cos \theta$  and  $\sin \theta$ , because the anti-symmetry of distribution, characterized by using  $\cos \theta$  only is violated due to difference in conditions for depository boundaries downstream and upstream. On the left side of equation (A.7.1) a term was omitted namely the flux outside the depository caused with appearance of the additional head drop,  $h_{s1}$ . This term is  $V_{s1} R/R$  and it is smaller than term  $V_{s1} R/d_b$  on the right side of equation (A.7.7).

## **Appendix 8** **Reactive Filter**

The qualitative distinction of reactive filter from a conventional PRB is characterized by the principle of barrier HC increase. The principle of barrier HC increase by means of simultaneous decrease of the filtration path length, namely RM using a thin layer between adjacent transport channels and filtration surface increase, namely filtration through transport channel surface, which exceed barrier front surface area 10-100 times. With account for this filtration surface increase and for RM layer thickness of 3 cm, that is 30-100 times smaller than usual thickness of a barrier, HC of PRB with channels can exceed that of a barrier filled with RM only and without channels approximately 1000 times, if necessary. For further explanation of this achievement, the condition that the pressure drop along the transport channel is small in

comparison with the entire pressure drop is useful. If this condition is satisfied the pressure drop between neighboring channels is slightly smaller than the entire pressure drop across the barrier. This condition can be easily satisfied with transport channel width exceeding 2-5 mm or by increasing pores in porous transport channel up to 2 mm. This provides the maximum filtration velocity through RM that is proportional to the pressure drop between the neighboring channels, i.e. proportional to almost entire pressure drop because they are almost equal at the condition aforesaid.

The maximum pressure drop across RM and consequently maximum HC is provided if the pressure in one channel is almost equal to the pressure before barrier and in the neighboring channel the pressure is equal to pressure after channel, i.e. near its back surface. This condition is easily provided as the first channel is connected with the space before barrier and is isolated from the space beyond barrier and as the second channel is isolated from the space before barrier and connected with the space beyond the barrier. In other words, the first channel has entrance within the barrier front surface and has no exit within the barrier back side. The groundwater entering the first channel filtrates as a whole through adjacent RM into the second channel. On the contrary, the second channel has no entrance within the barrier front side and has exit within the barrier back side. GW enters in second channel through RM only, i.e. the second channel is filled with cleaned water which flows out from barrier. The channels array is arranged as consisting of those pairs of channels. The comparison of the entire GW stream through 2 barrier with the same length  $l$ , height  $H$  and thickness  $d_b$  and with the same RM and  $K_{RM}$ , one without the channels and second with channels characterizes the stream enhancement due to channel incorporated into the barrier and the possibility of bypassing prevention

$$j_b = lH \frac{H_{RM}}{d_b} \Delta p \quad (\text{A.8.1})$$

$$j_{bch} = S_{bch} \frac{H_{RM}}{d_{RM}} \Delta p \quad (\text{A.8.2})$$

where the entire surface of transport channels:

$$S_{bch} = n2d_b H \quad (\text{A.8.3})$$

where  $2d_b H$  is the surface of one channel and the total number of channels is given as:

$$n = l / d_{RM} \quad (\text{A.8.4})$$

Using equations (A.8.1) - (A.8.4), we obtain:

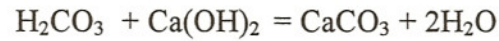
$$\frac{j_{bch}}{j_b} = \left( \frac{d_b}{d_{RM}} \right)^2 \quad (\text{A.8.5})$$

This increase of entire HC of a barrier is illustrated for different  $n$  values in Fig. 22. According to our measurements (Table 3), HC of RM after its aging is less than soil HC approximately 10 times. This 10 times decrease in local HC can be compensated using reactive filter with  $n = 3$  channels per 1 meter of barrier length. As the filtration surface can be increased 30 times using TCH technology, the filtration flux density (through the channel "walls") can be decreased 30 times in the barrier with TCH in comparison with that in conventional barrier. Therefore, the residence time for a contaminant reduction is preserved although RM layer thickness decreases 30 times. It occurs because the filtration velocity decreases 30 times. The contaminant amount accumulated in the film per  $\text{cm}^2$  of its surface will be 30 times smaller than

at the conventional design of a barrier. But this amount per  $\text{cm}^2$  of the front surface of a barrier with TCH will be the same as in case of barrier of conventional design, because the filtration surface is extended 30 times.

### **Appendix 9** **Calcite Precipitation**

The formation of  $\text{CaCO}_3$  deposit is possible due to the reaction:



It is possible that  $\text{CaCO}_3$  micro-crystal can block the barrier. This reaction demonstrated that  $\text{Ca}(\text{OH})_2$  disappears, i.e. pH decreases. On the other hand, the initial high pH enhances calcite precipitation.

**FIGURES**

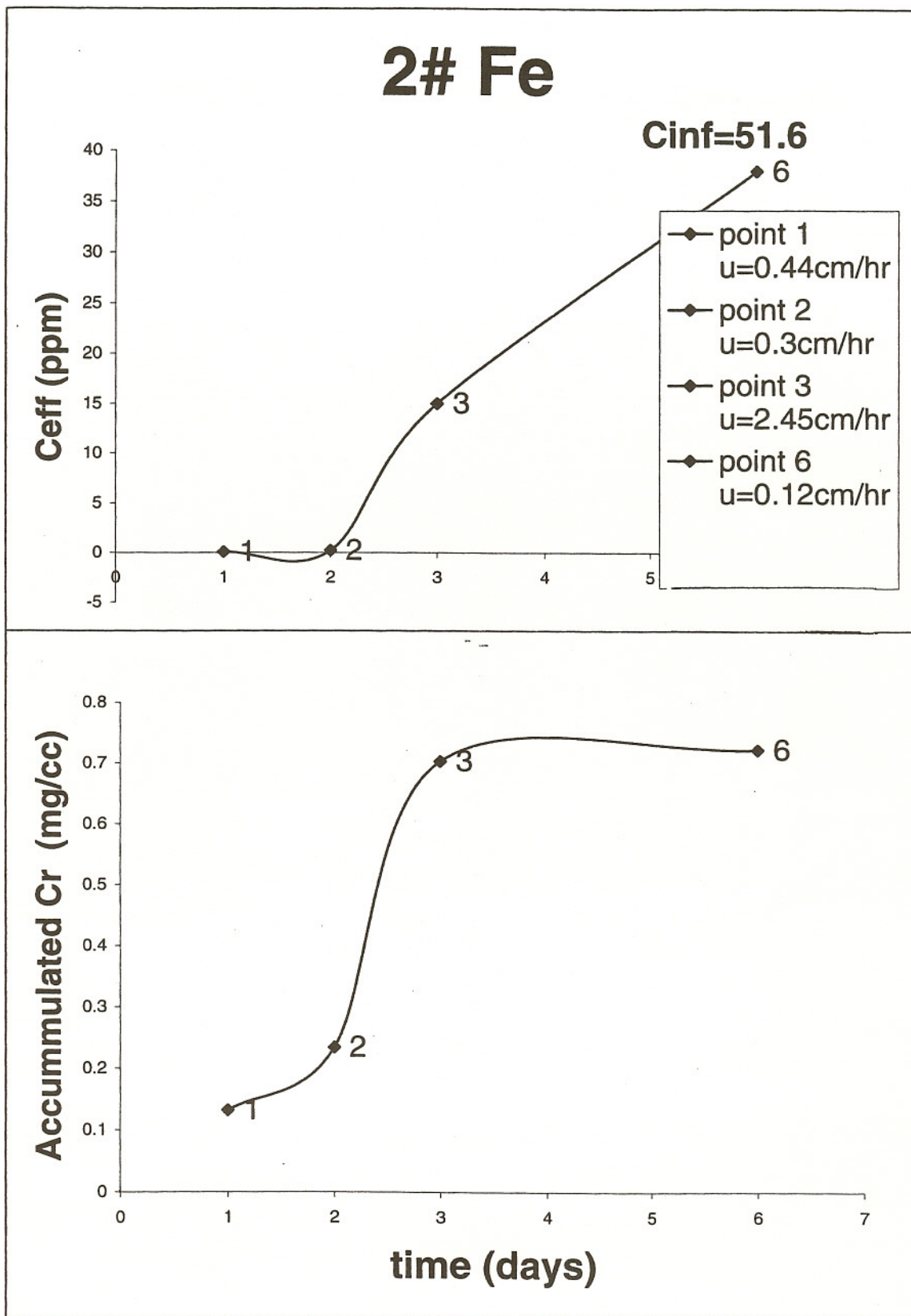


Fig. 1. Effluent concentration ( $c_{eff}$ ) and accumulated Cr(III) as a function of time for iron 2 as reactive media ( $c_{inf} = 51.6$  ppm)

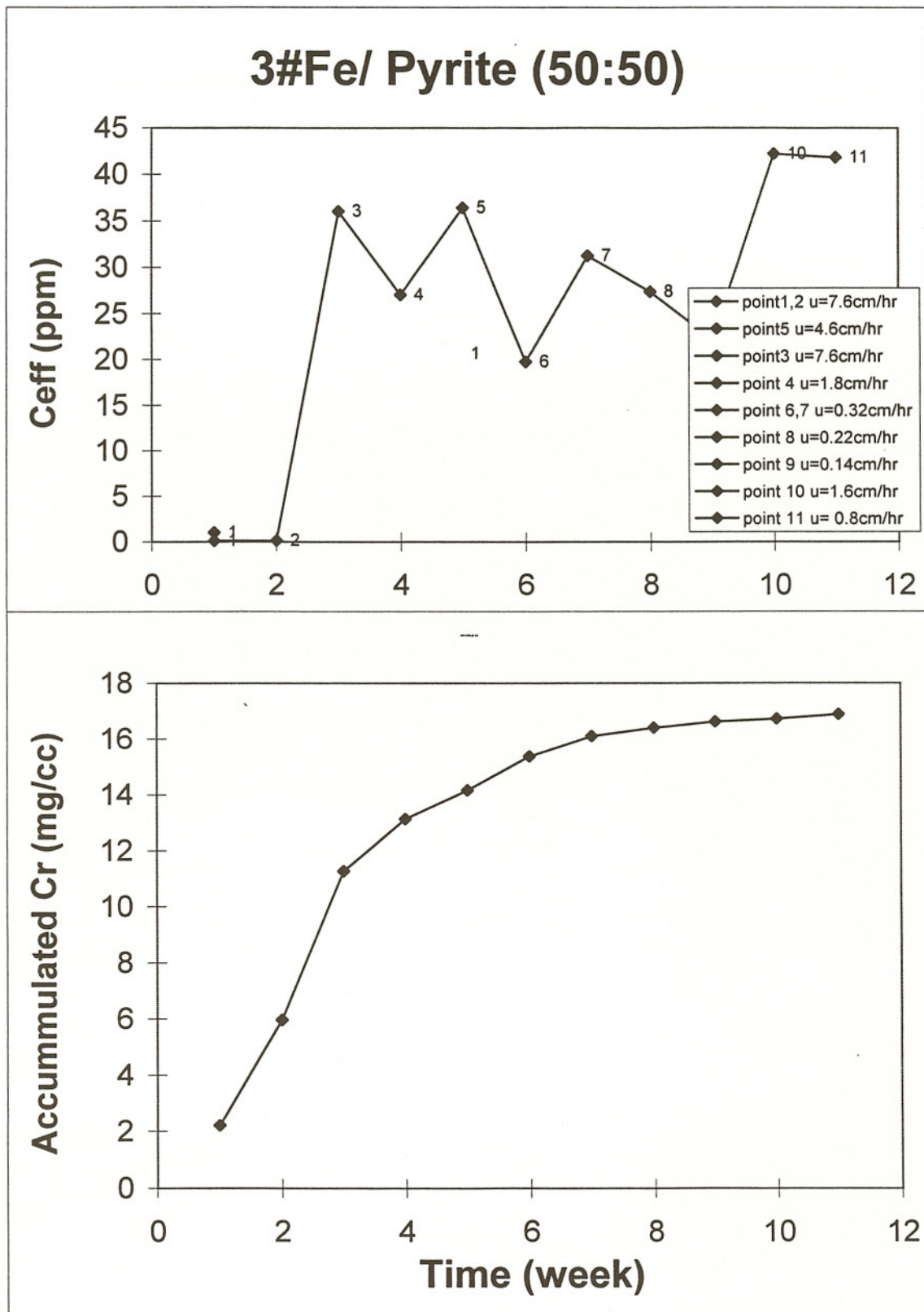


Fig. 2. Effluent concentration ( $c_{eff}$ ) and accumulated Cr(III) as a function of time for iron 3-pyrite (50:50) mixture as reactive media ( $c_{inf} = 51.6$  ppm)

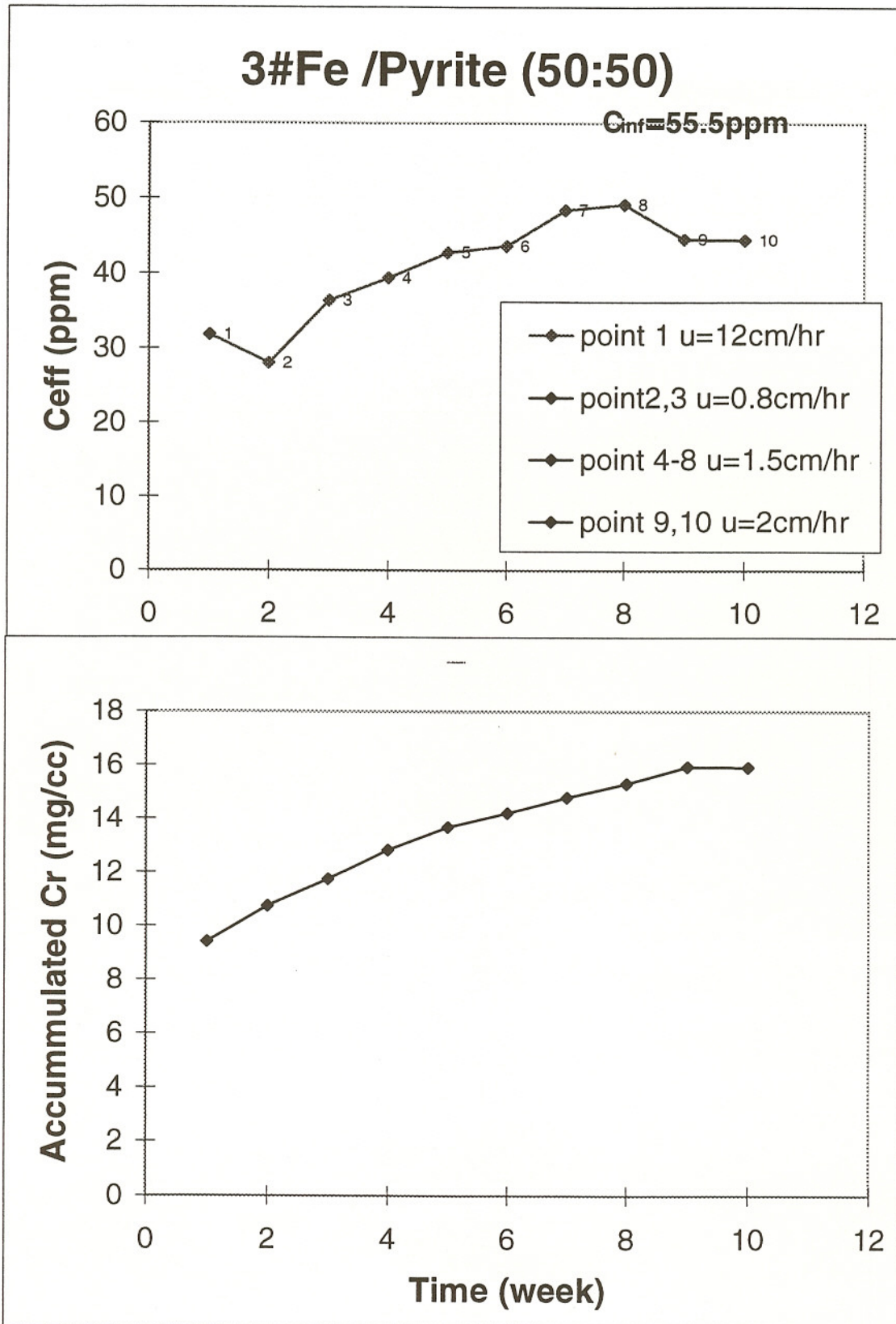


Fig. 3. Effluent concentration ( $c_{eff}$ ) and accumulated Cr(III) as a function of time for iron 3-pyrite (50:50) mixture as reactive media ( $c_{inf} = 55.5 \text{ ppm}$ )

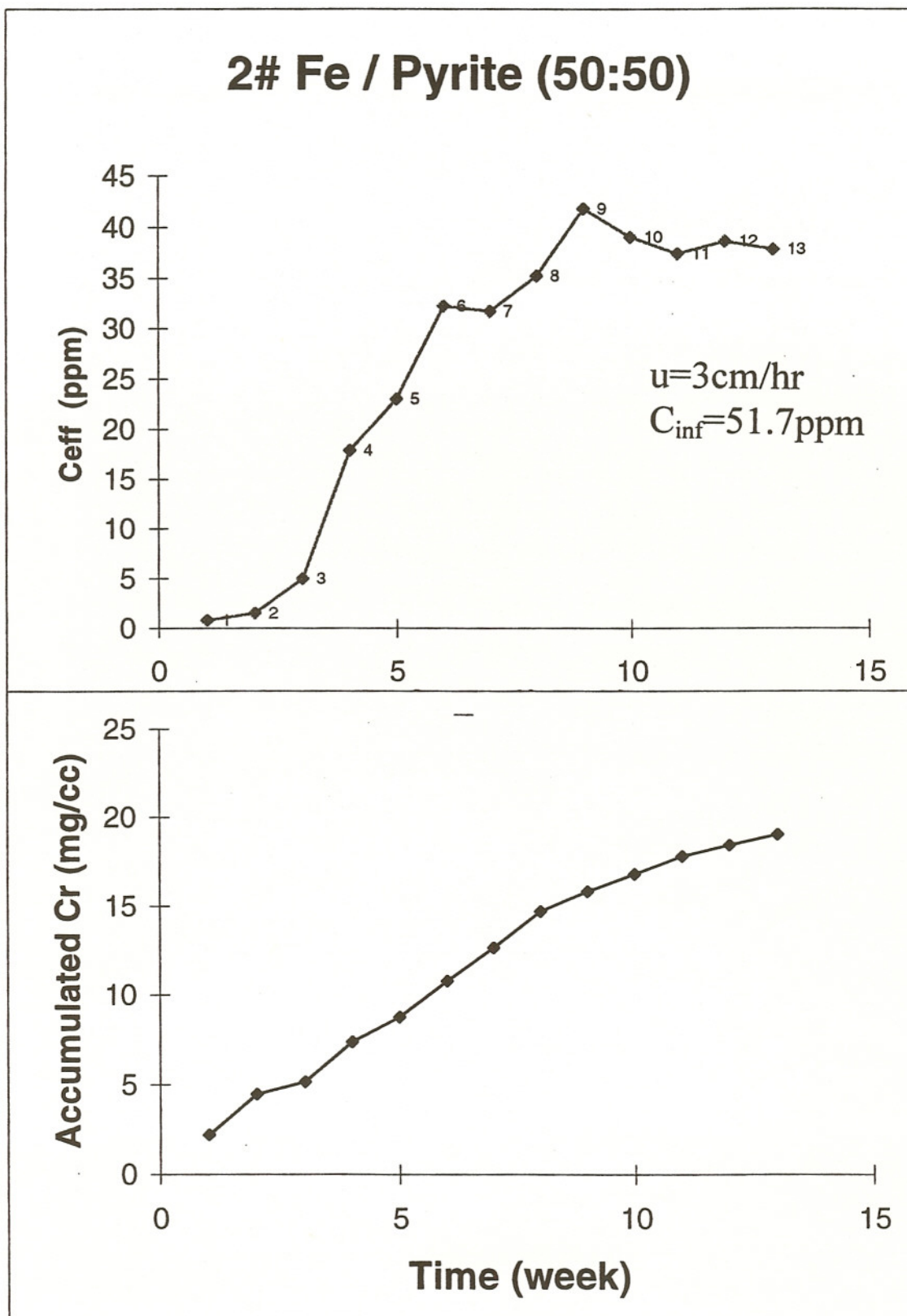


Fig. 4. Effluent concentration ( $c_{\text{eff}}$ ) and accumulated Cr(III) as a function of time for iron 2-pyrite mixture as reactive media ( $c_{\text{inf}} = 51.7 \text{ ppm}$ ,  $u = 3 \text{ cm/hr}$ )

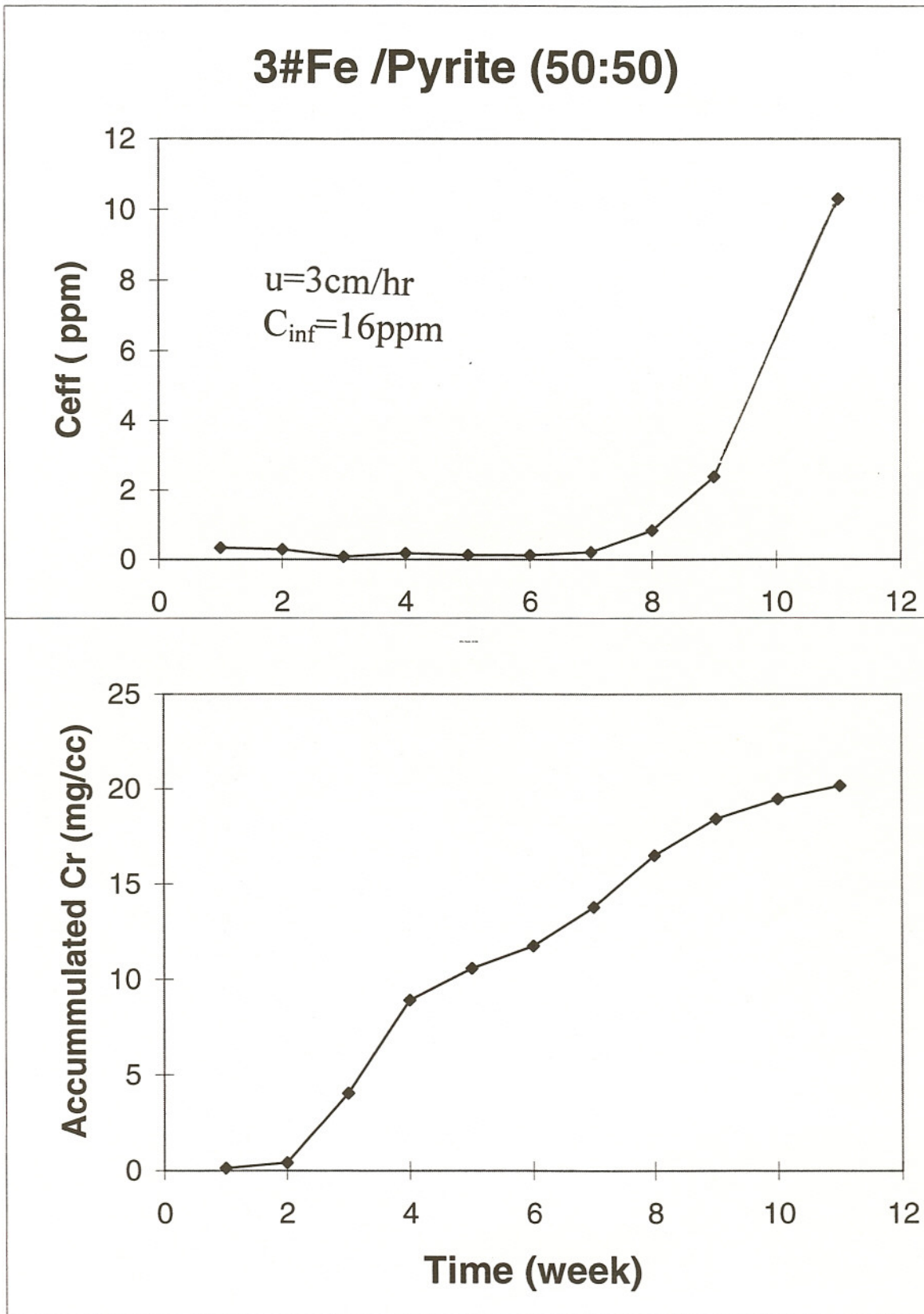


Fig. 5. Effluent concentration ( $c_{eff}$ ) and accumulated Cr(III) as a function of time for iron 3-pyrite mixture as reactive media ( $c_{inf} = 16$  ppm,  $u = 3$  cm/hr)

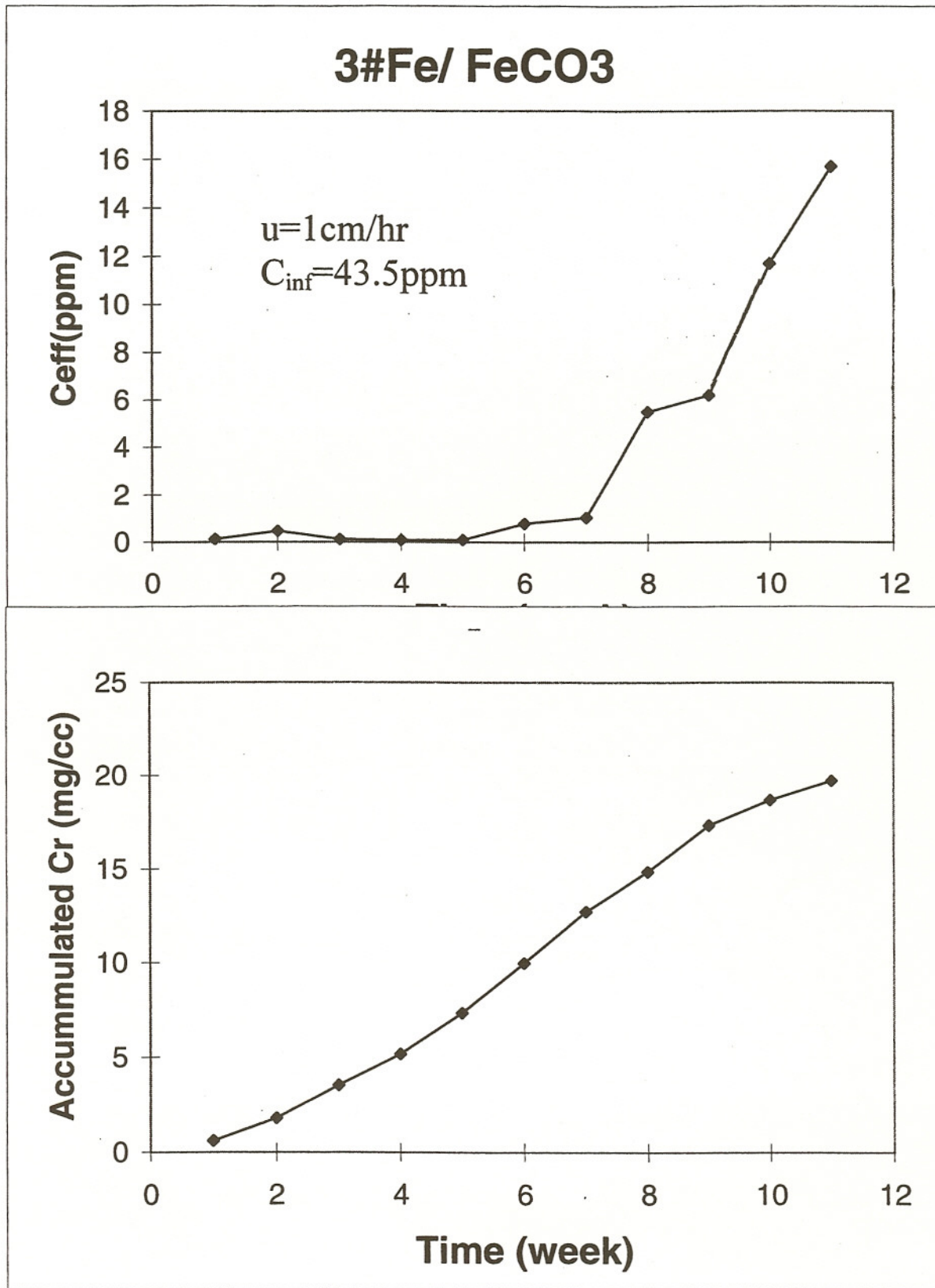


Fig. 6. Effluent concentration ( $c_{eff}$ ) and accumulated Cr(III) as a function of time for iron 3-FeCO<sub>3</sub> mixture as reactive media ( $c_{inf} = 43.5 \text{ ppm}$ ,  $u = 1 \text{ cm/hr}$ )

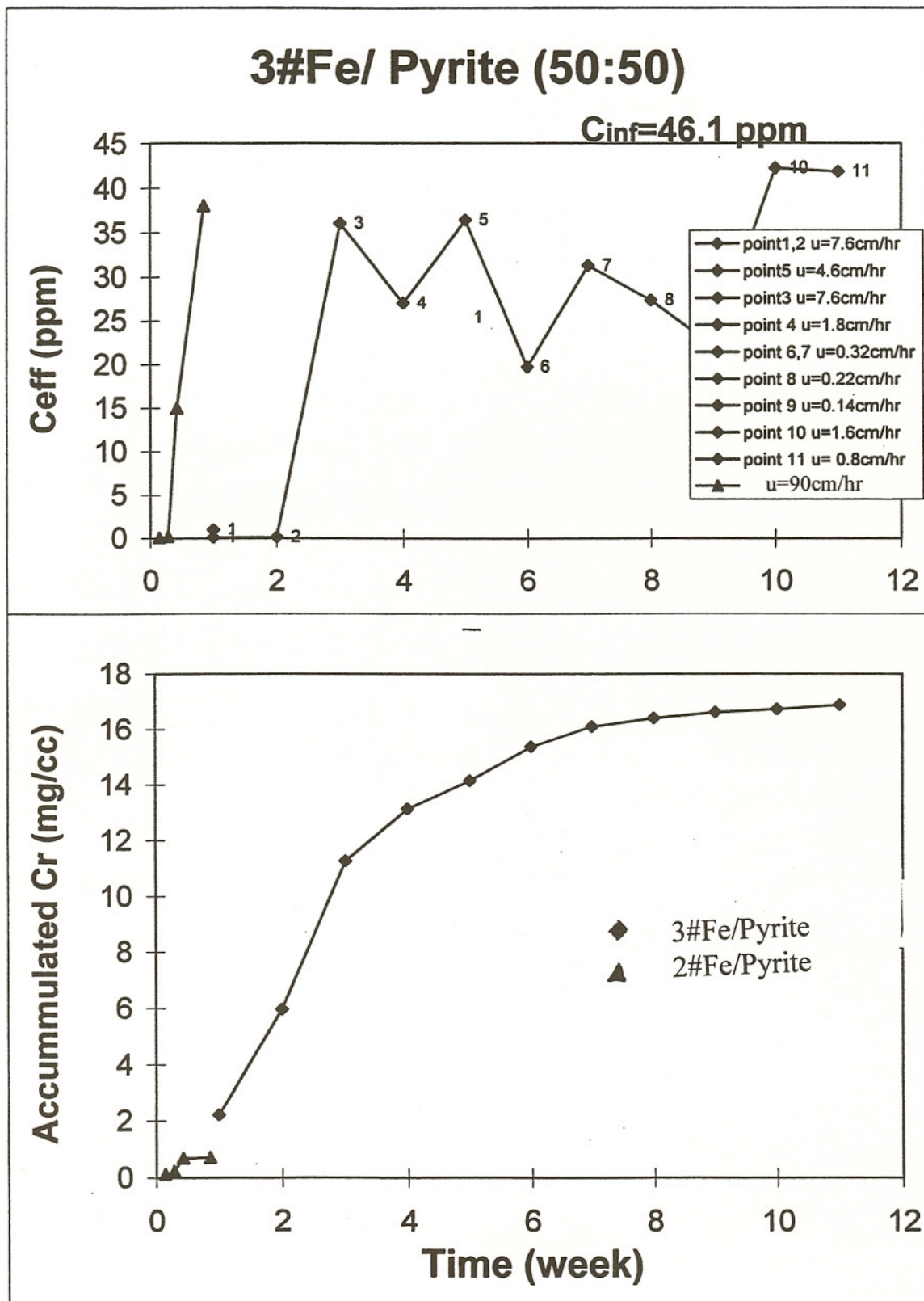


Fig. 7. Effluent concentration ( $c_{eff}$ ) and accumulated Cr(III) as a function of time for iron 3-pyrite and iron 2-pyrite mixtures as reactive media

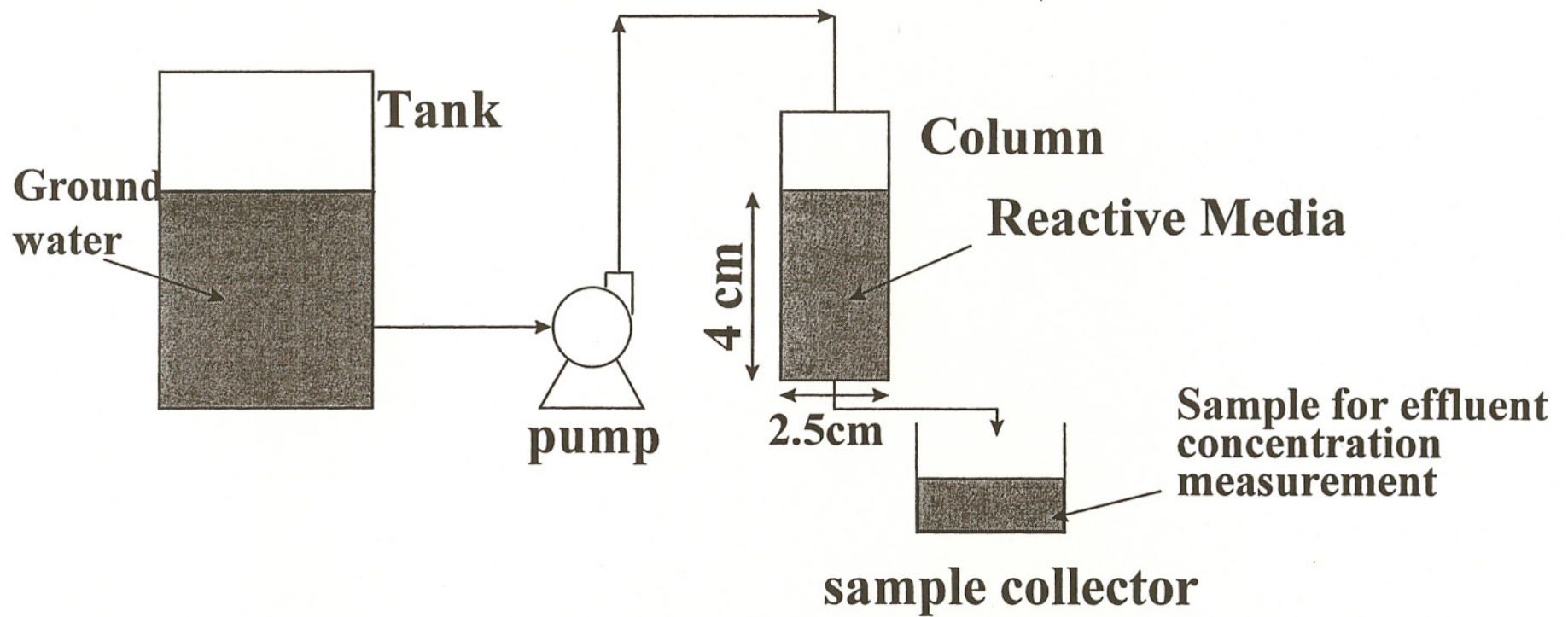
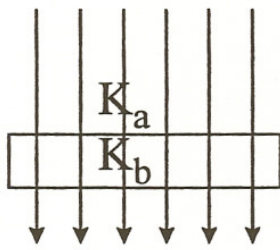
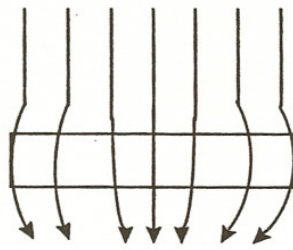


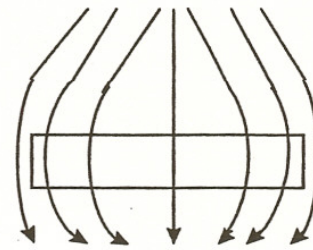
Fig. 8. Experimental set-up used for long term measurement of reduction rate decrease caused by reduced chromium accumulation



$K_b = K_a$   
No streamlining



$K_a > K_b > (0.3-0.5)K_a$   
Streamlining is weak



$K_b < 0.1 K_a$   
Streamlining is strong

Fig. 9. Streamlining around a barrier --- Three scenarios

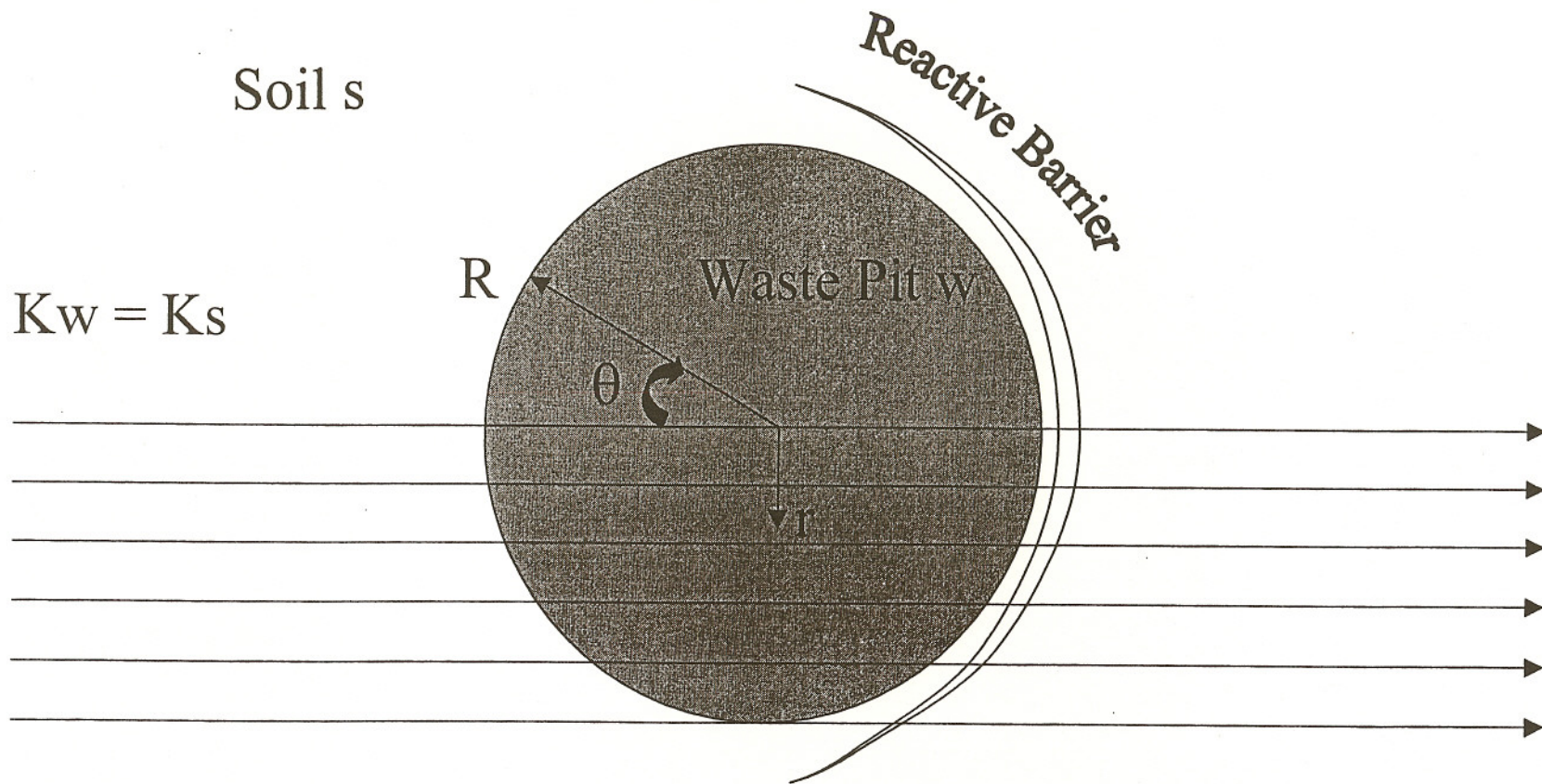
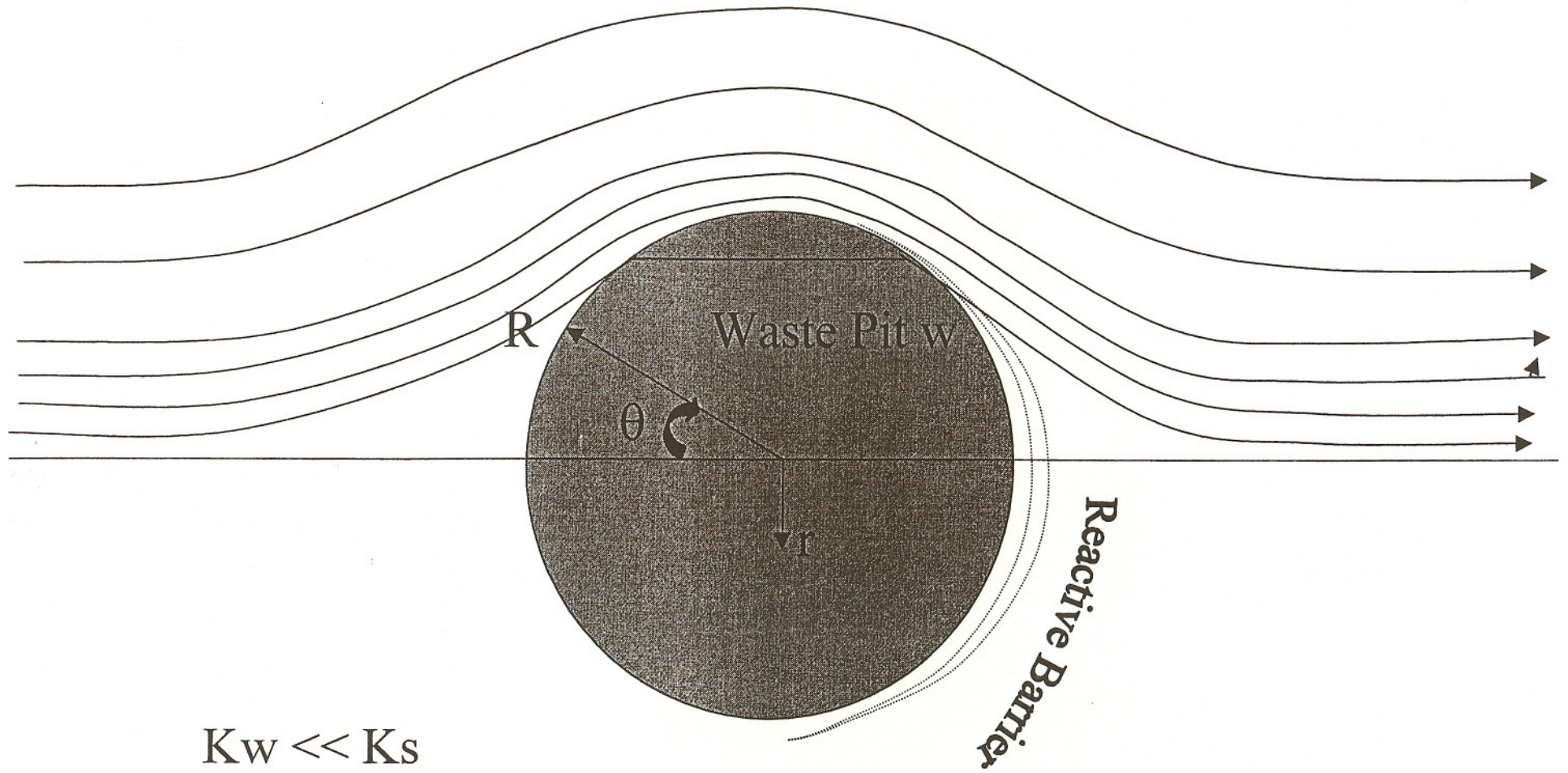


Fig. 10a. Flow around and within a waste depository --- For  $K_w = K_s$ , the flow field is characterized by straight lines

Soil s



$$K_w \ll K_s$$

Fig. 10b. Flow around and within a waste depository --- For  $K_w < K_s$ , the flow upstream of depository is divergent and downstream of it is convergent

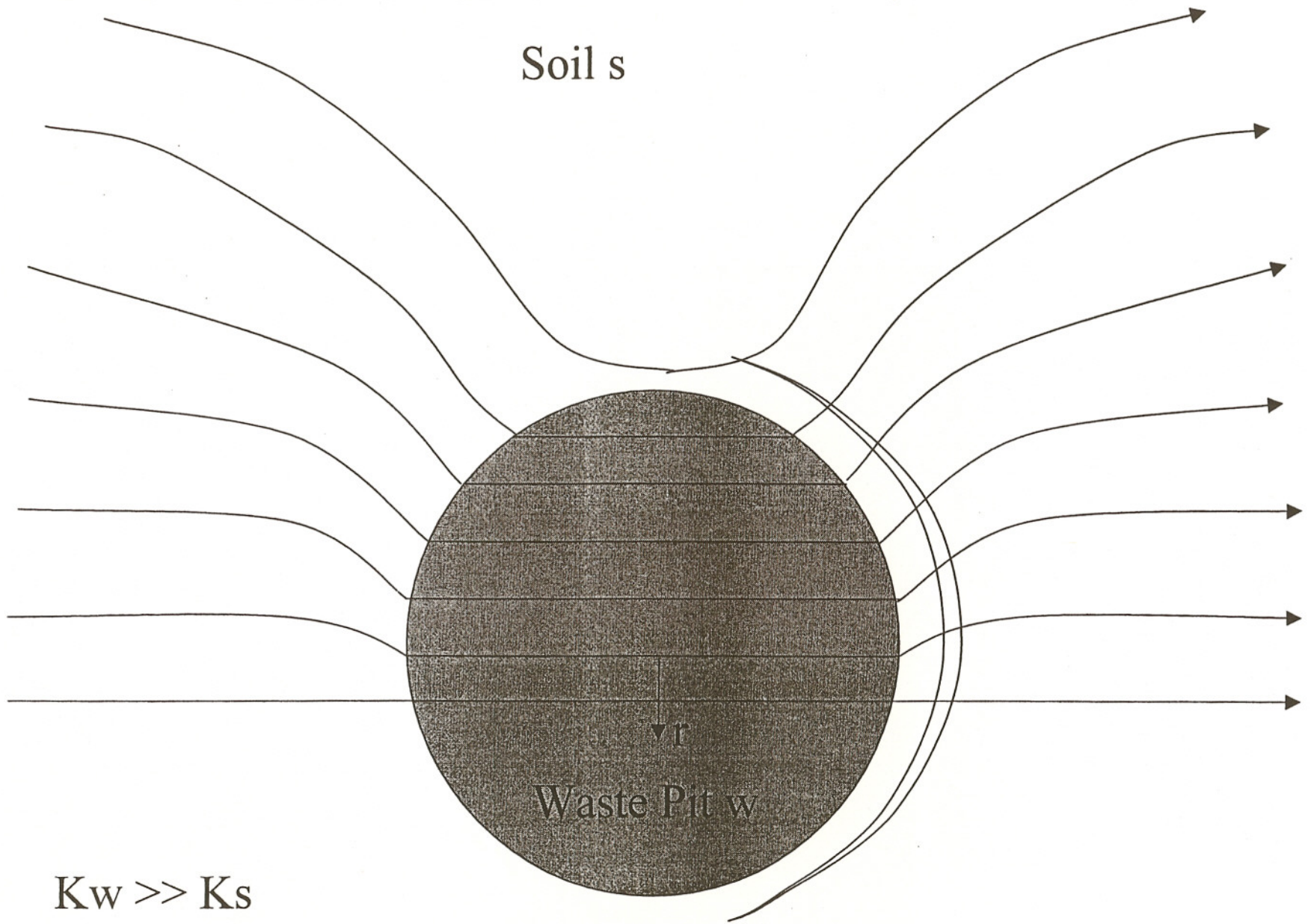
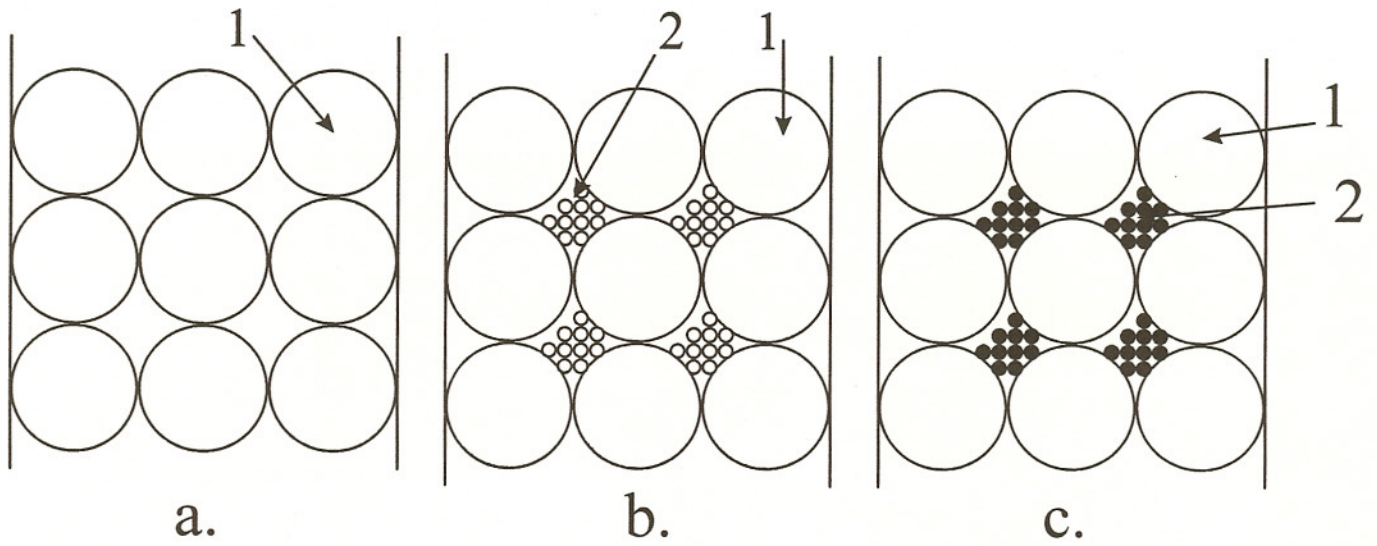
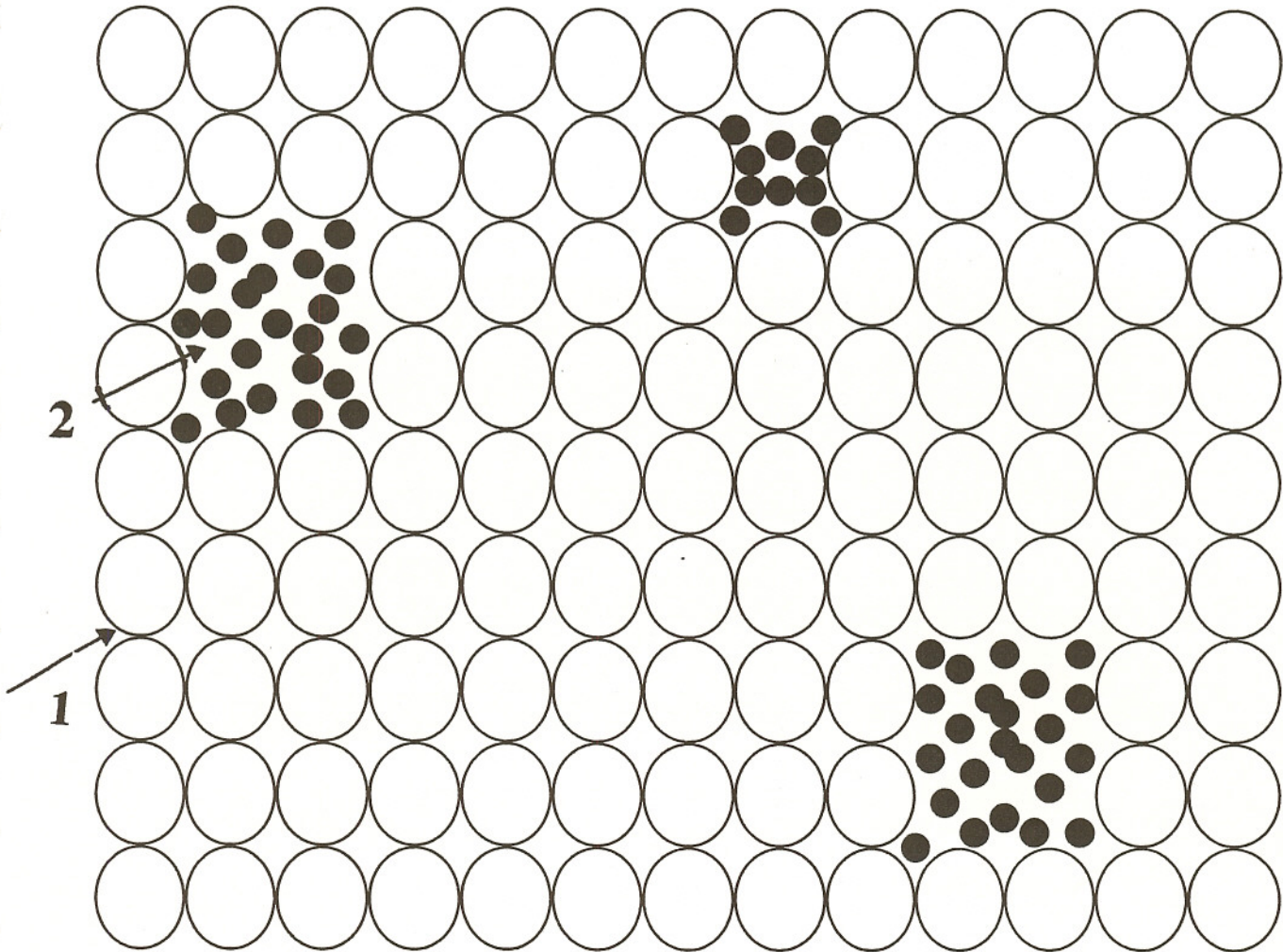


Fig. 10c. Flow around and within a waste depository --- For  $K_w > K_s$ , the flow upstream of depository is convergent and downstream of it is divergent



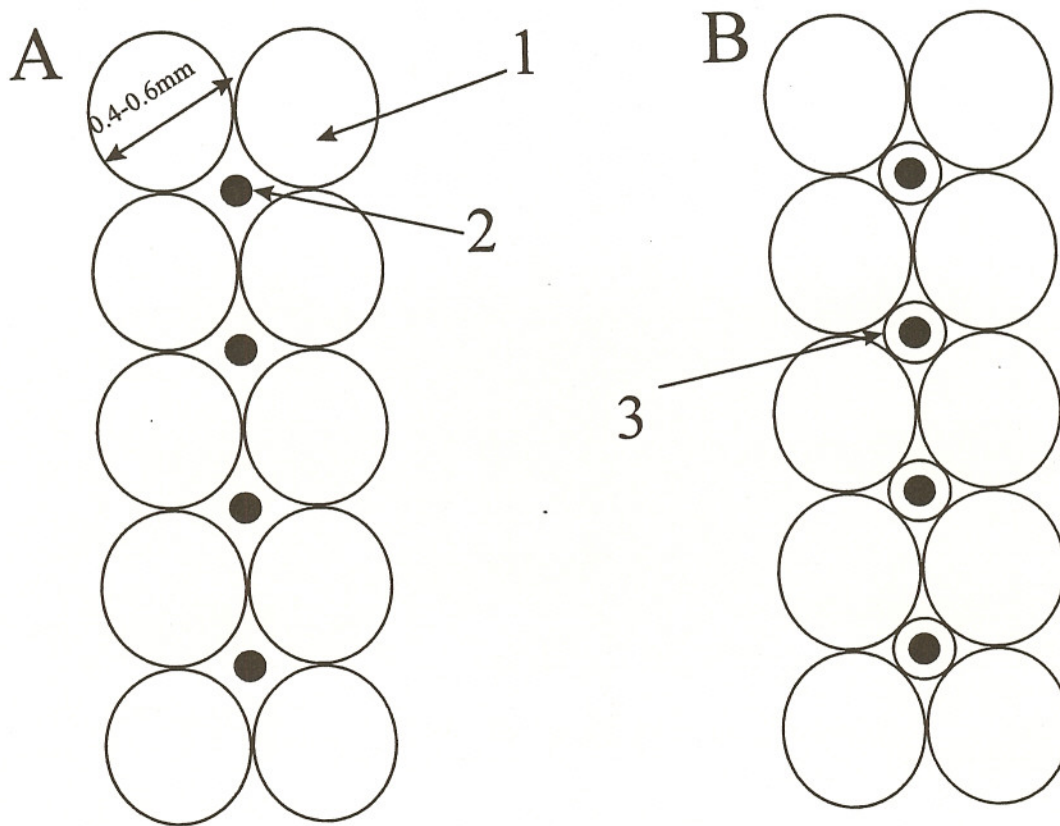
- a. The porosity is maximum in the packed bed of monodisperse particles.
- b. The porosity decreases in the polydisperse powder case because the smaller particles occupy space in pores between larger particles. There is a small space for RM in pores of a polydisperse soil (sand). [1. Soil large particles, 2. Soil small particles]
- c. After removal of fine fractions from soil, the pores between larger soil particles increase and the space for RM and for water flow increases. The larger the dimension of coarse particles remaining after small fraction separation, the larger will be the RM volume fraction and therefore, larger HC. [1. Soil (sand) large particles, 2. RM particles occupy space remaining after small soil particle removal]

Fig. 11. Importance of removing smaller soil particles for increasing RM volume fraction in RM/sand mixture



The complete separation of RM particles and their uniform distribution between sand particles is not achieved at weak mixing. RM particle portions (RMPP) with dimensions of 0.2-0.8 mm are preserved and randomly distributed within sand particles. Addition of RM in the form of RMPP to sand causes a minor decrease in hydraulic conductivity because the majority of transport channels (pore sequence) for water transport is preserved. [1. Sand particles, 2. RM particle portions consisting of 10-1000 RM particles]

Fig. 12a. Weak vs. Almost ideal mixing --- Schematic for weak mixed RM with almost monodisperse fraction of sand (soil)

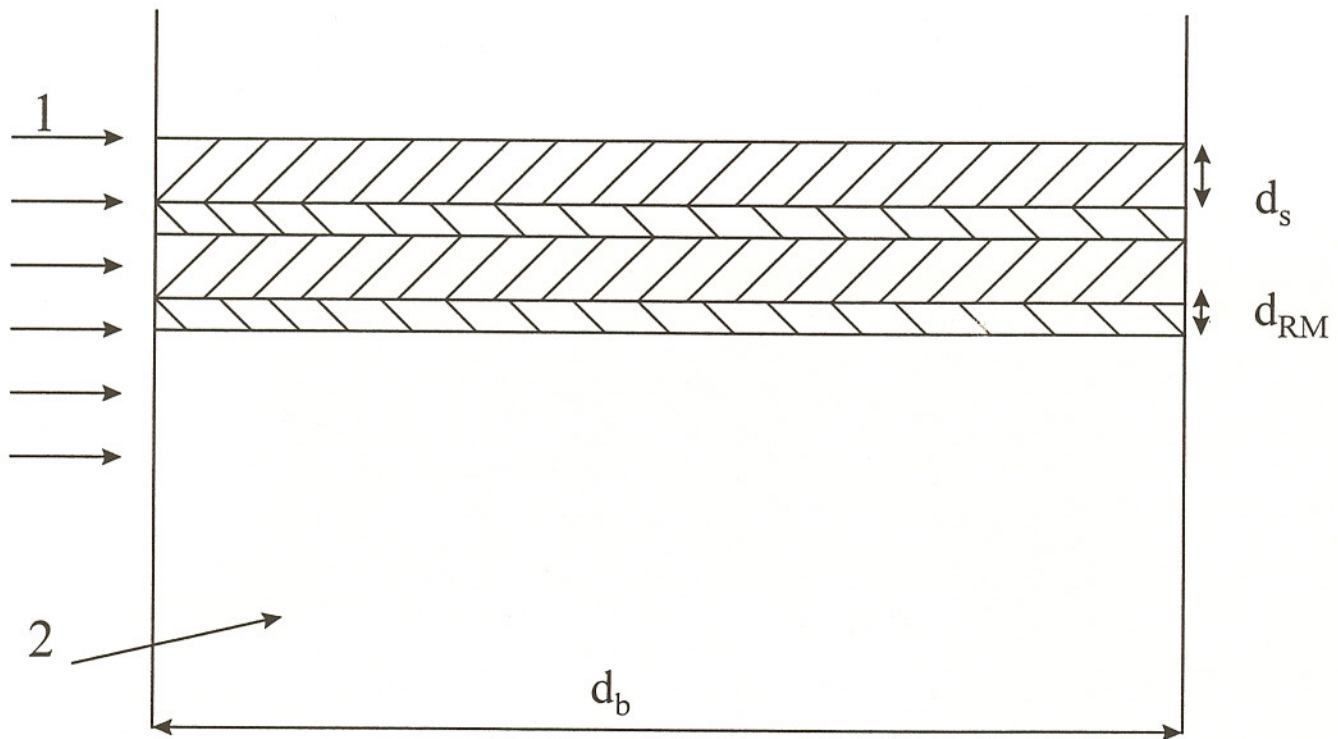


A. Sand with narrow size distribution and particles' dimensions 0.4-0.6 mm. Pores filled with RM particles with dimensions around 0.1 mm.

B. Pores are clogged mainly with either reduced chromium compound or with calcium deposit.

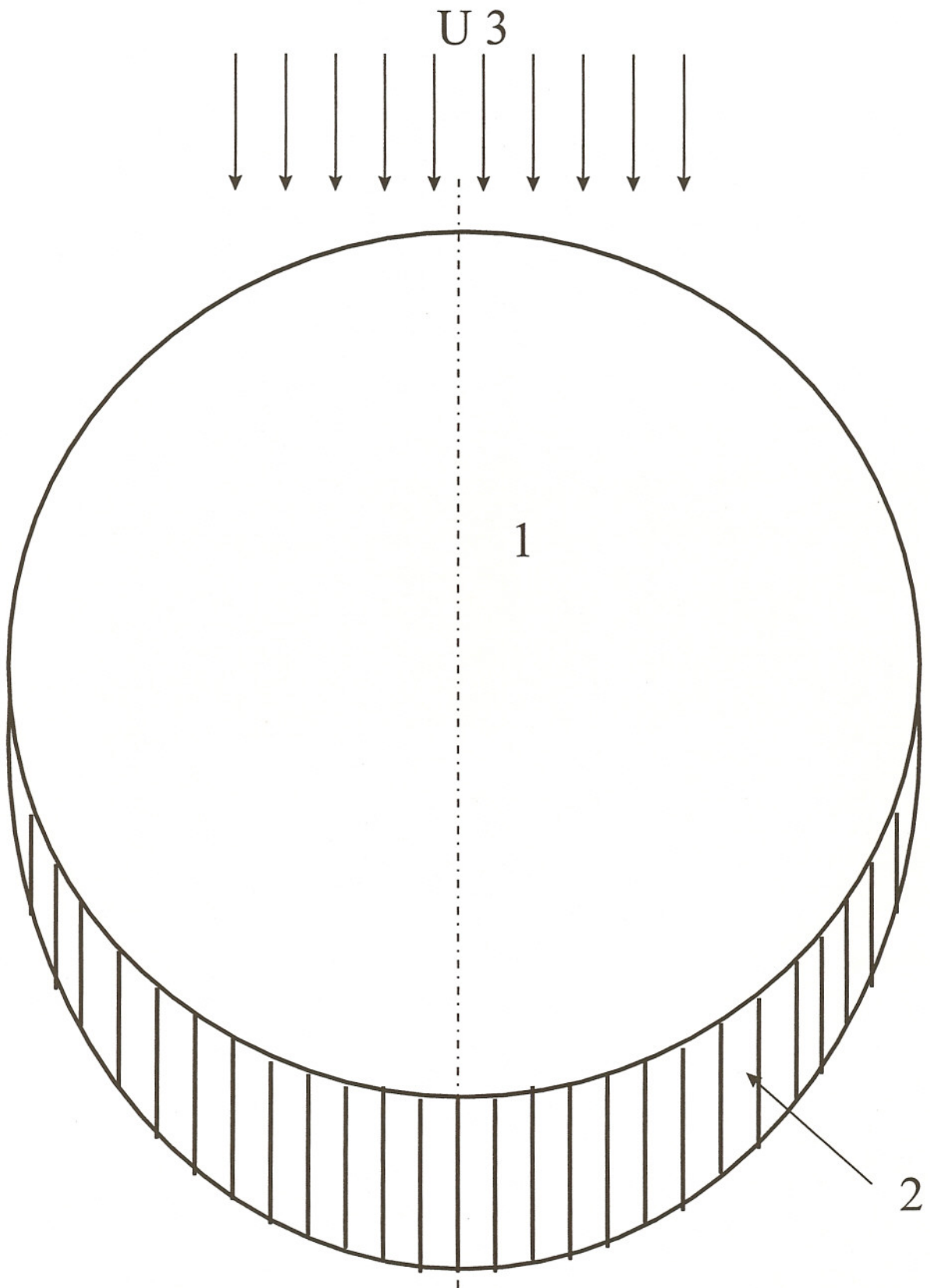
Almost every pore between sand particles is filled with a particle of RM that causes strong retardation of GW flow. A further decrease in hydraulic conductivity is caused by the decrease in free space in pores for GW flow, as reduced chromium compound or calcium deposit covers RM particle surface. This kind of mixing is not favorable for a barrier installation using RM/sand (soil) mixture. [ 1. Sand, 2. RM particle, 3. Deposit]

Fig. 12b. Weak vs. Almost ideal mixing --- Schematic illustration of almost ideal mixed RM with almost monodisperse sand (soil) fraction



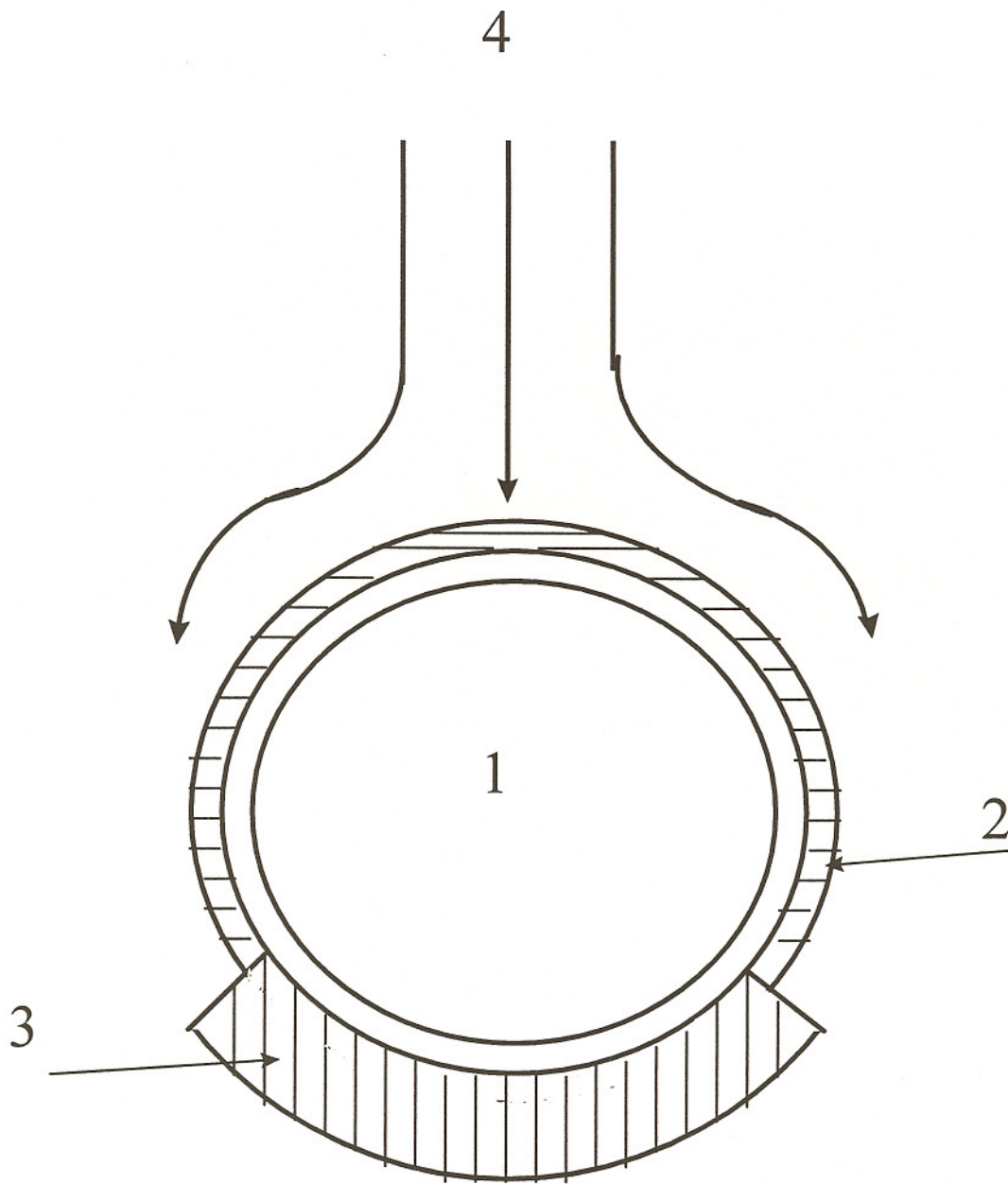
The layer of soil coarse fraction or coarse sand has a large HC decline that provides a large HC of barrier as a whole and prevents bypassing. This high barrier HC is preserved even at very strong HC decline within RM layer caused by chromium accumulation because GW moves mainly within sand layer and HC declination occurs within RM layer. During the residence time, chromium diffuses from sand layer into RM layer where its reduction and accumulation takes place. [1. GW stream, 2. PRB layered structure,  $d_s$  = soil layer thickness,  $d_{RM}$  = RM layer thickness,  $d_b$  = PRB thickness]

Fig. 13. Schematic of RM/soil layered structure



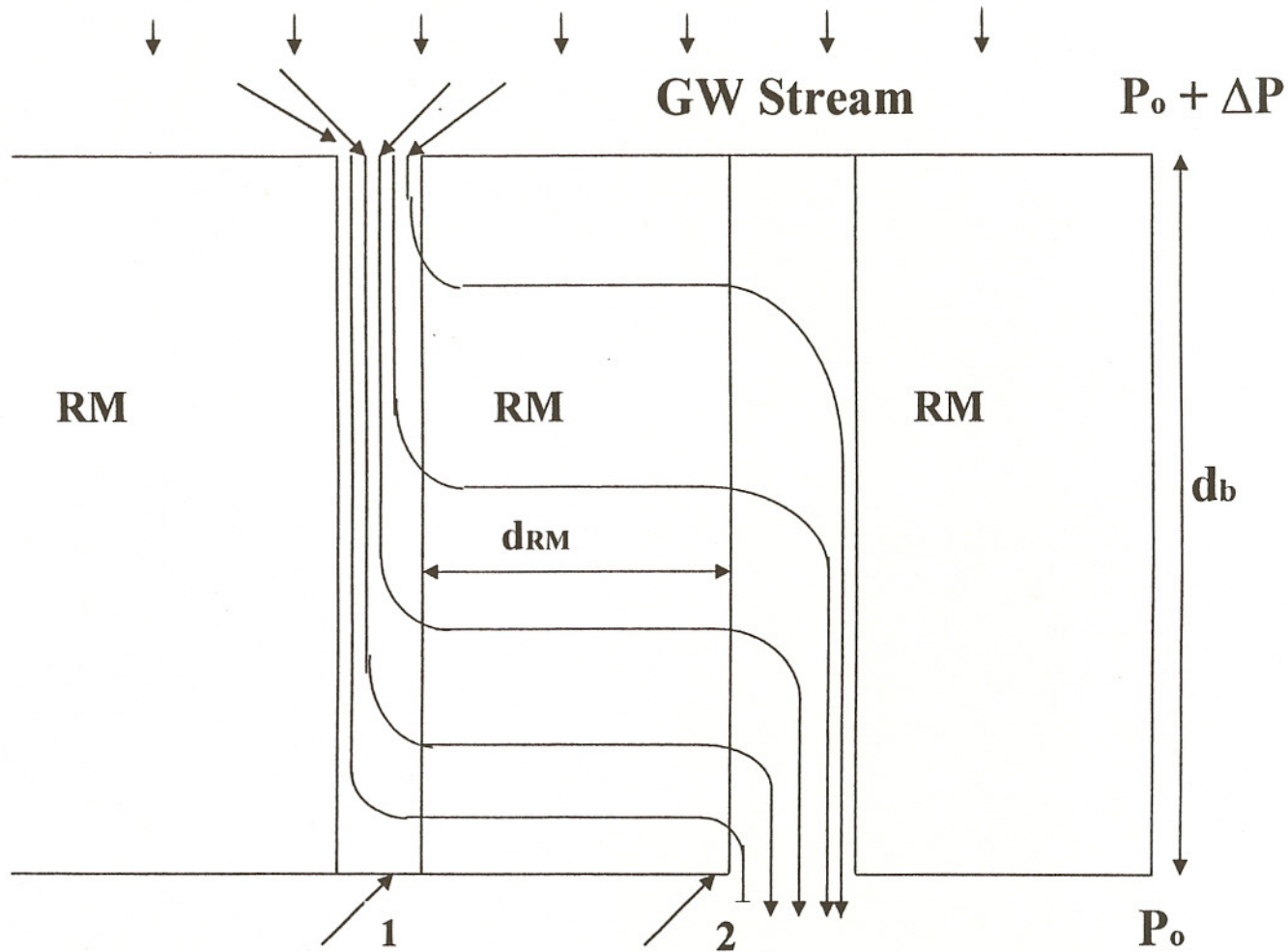
[1. Depository, 2. Barrier of variable thickness, 3. Groundwater stream velocity]

Fig. 14. Schematic of variable thickness barrier in continuous configuration



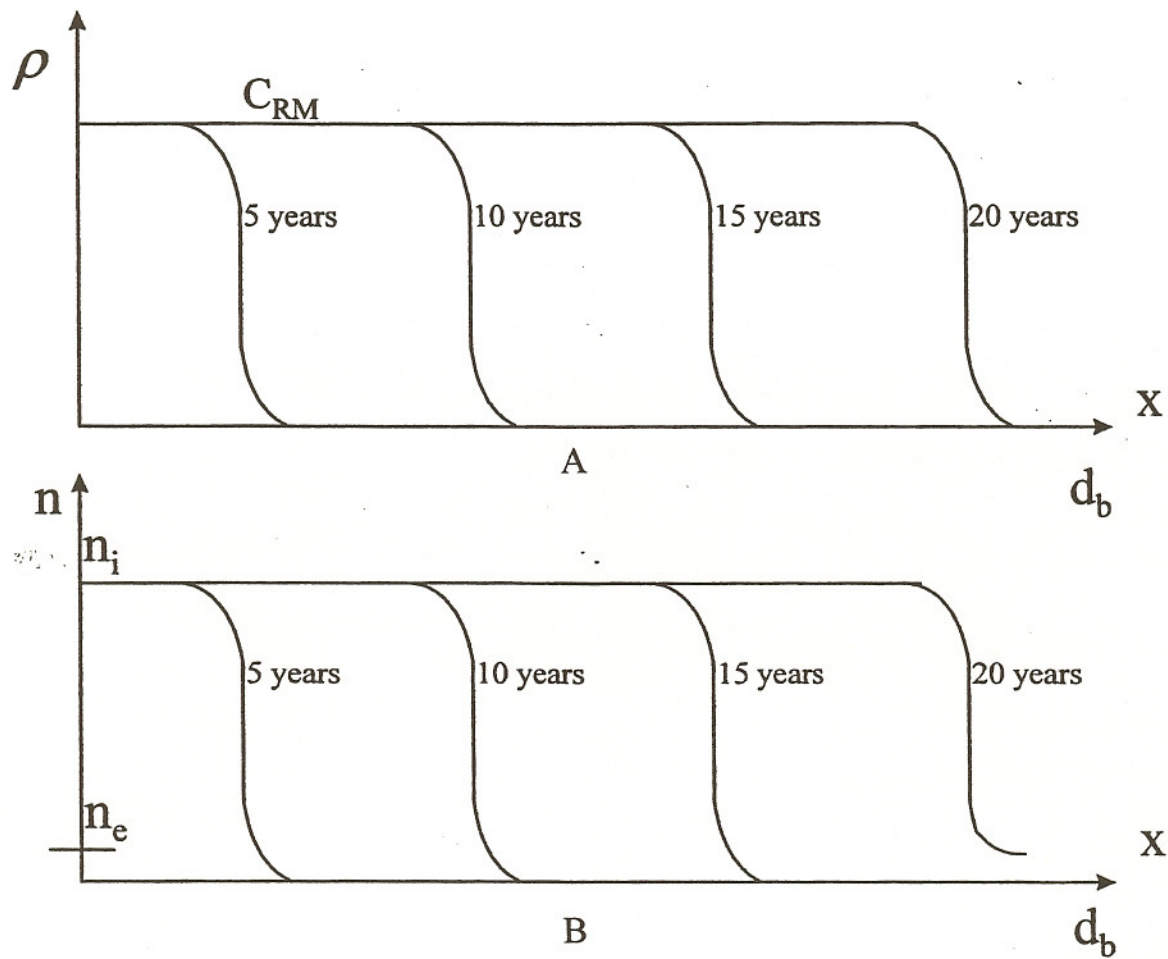
[1. Depository, 2. Upstream cutoff wall, 3. PRB, 4. GW stream]

Fig. 15. Schematic of barrier configuration supplemented with upstream cutoff walls



The filtration area increases and the hydrodynamic resistance decreases by the use of transport channels in PRB.  
 [1. Incoming GW channel, 2. Cleaned water channel, 3.  $\Delta P$ , barrier pressure drop, 4.  $d_b$ , barrier thickness]

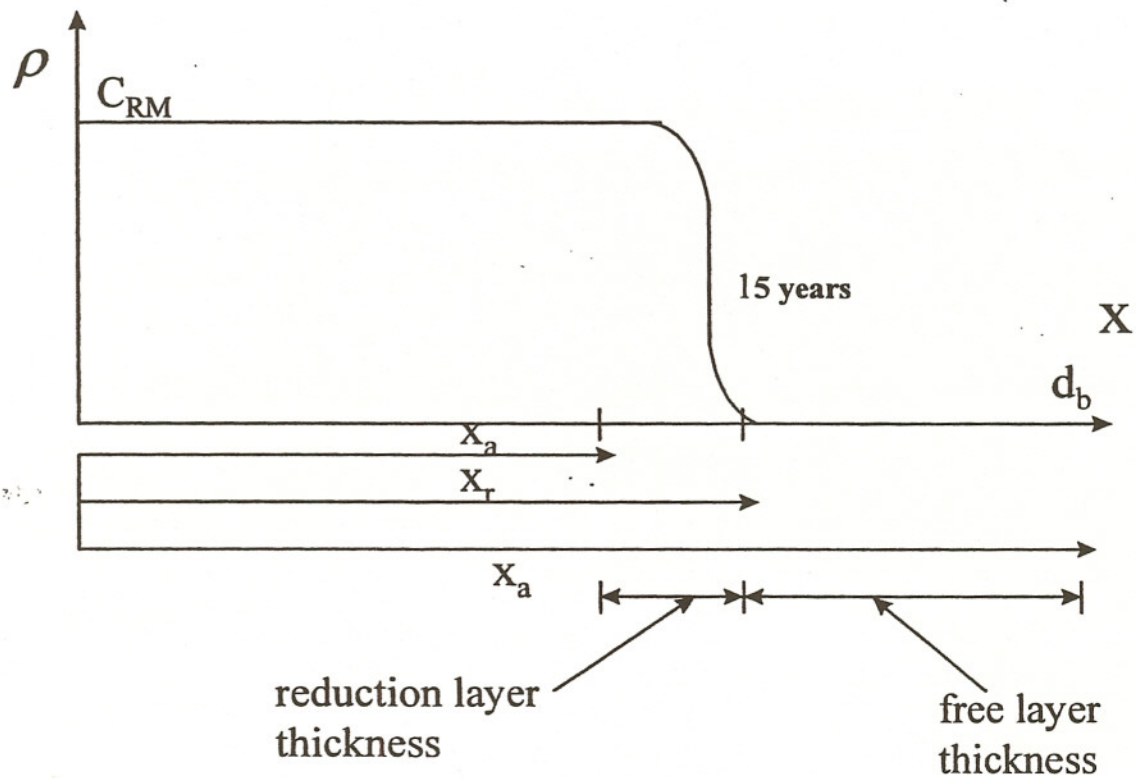
Fig. 16. Schematic of PRB with channels



- A. The accumulated Cr(III) mass distribution,  $\rho(x)$  across a barrier with thickness,  $d_b$  for duration from 5 to 20 years; 'x' is the distance from the barrier front (upstream) surface.
- B. The dissolved chromium distribution  $n(x)$  across the barrier.  $n_{x=0} = n_i$ ,  $n_{x=d} = n_e$ ,  $n_i$  and  $n_e$  are the influent and the effluent concentrations.

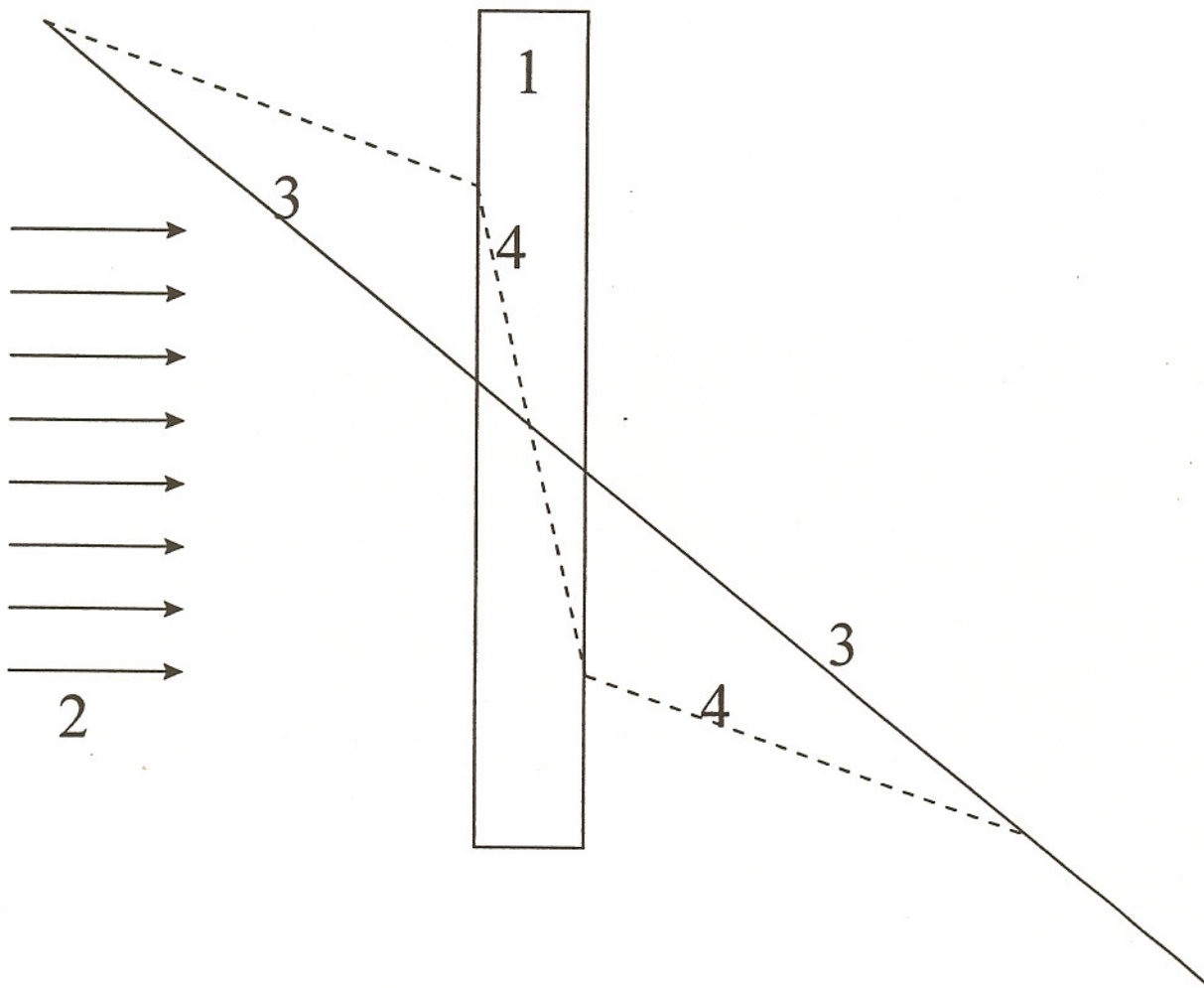
The complete passivation zone with the maximum accumulated chromium,  $\rho_{max}$  is seen in Fig. 'A'. Its length extends at constant rate. There is no dissolved chromium reduction within the passivation layer. As a result, the influent concentration is preserved within this passivated layer. After 20 years, the completed passivated zone comprises the entire barrier volume. The reduction takes place in the thin zone near the back (downstream) side of the barrier and correspondingly, concentration ( $n$ ) decreases in this thin zone only.

Fig. 17a. Illustration of reactive barrier performance during 20 years



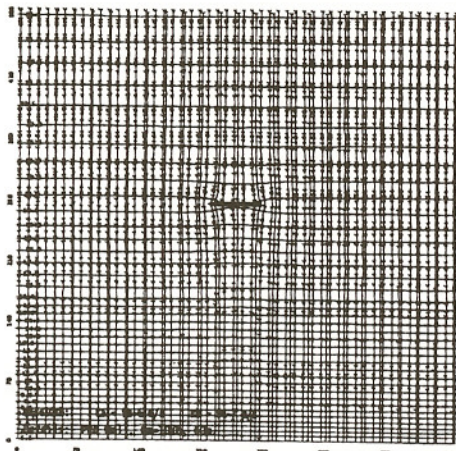
[ $X_a(t)$  = current thickness of accumulation layer,  $X_r(t)$  = the mobile boundary between reduction layer and third layer,  $(X_r - X_a)$  = the thickness of the reduction layer,  $(d_b - X_r)$  = the thickness of third (almost free) layer]

Fig. 17b. Three layer model of chromium accumulation dynamics in PRB

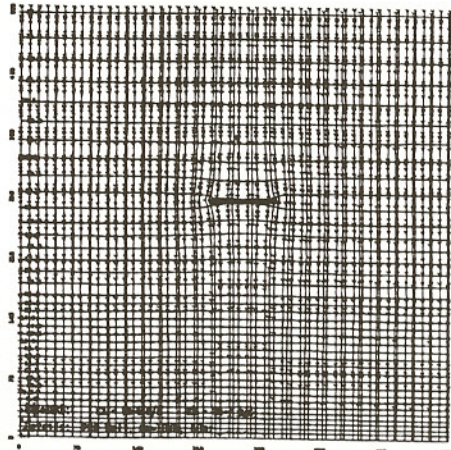


Hydraulic head distribution before, inside and behind a barrier. [1. Barrier, 2. GW stream, 3. Hydraulic head distribution at  $K_b = K_a$ , 4. Hydraulic head distribution at  $K_b < K_a$ ,  $K_a$  = hydraulic conductivity of aquifer,  $K_b$  = hydraulic conductivity of barrier]

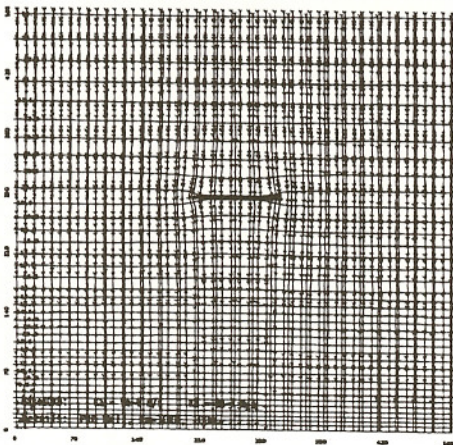
Fig. 18. Schematic illustration of bypassing mechanism



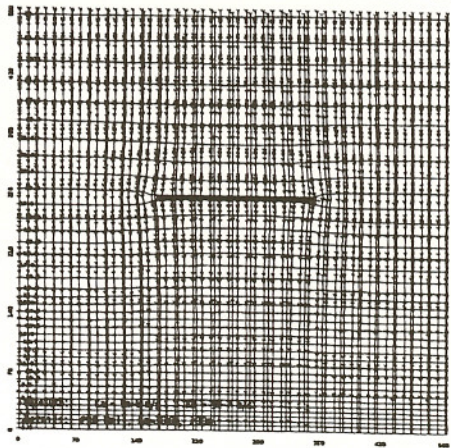
(s)  $Ka=10Kb$ , Length 60



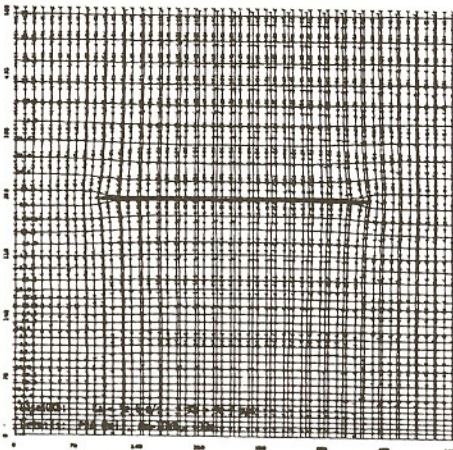
(t)  $Ka=10Kb$ , Length 80



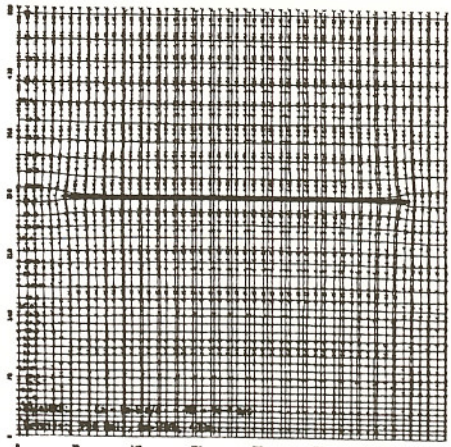
(u)  $Ka=10Kb$ , Length 100



(v)  $Ka=10Kb$ , Length 200



(w)  $Ka=10Kb$ , Length 300



(x)  $Ka=10Kb$ , Length 400

Fig. 19. Visual modflow runs for varying lengths of barrier [17]

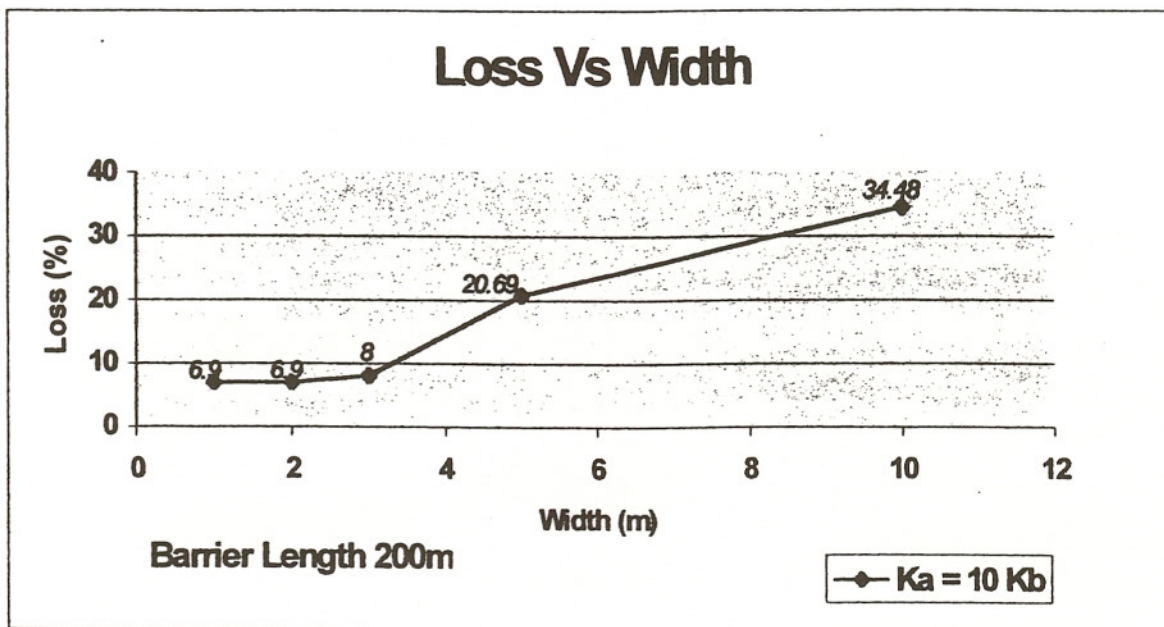


Fig. 20. Contaminant loss as a function of barrier width (barrier length = 200 m and  $K_a = 10 K_b$ )

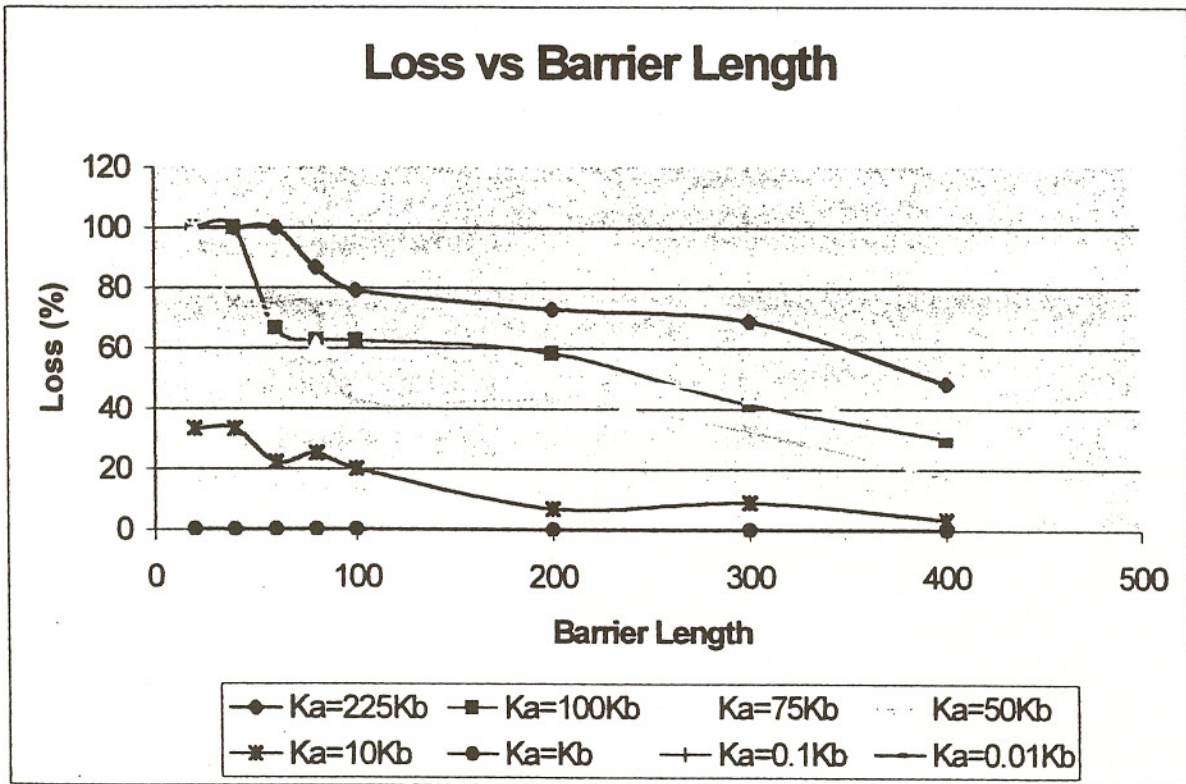
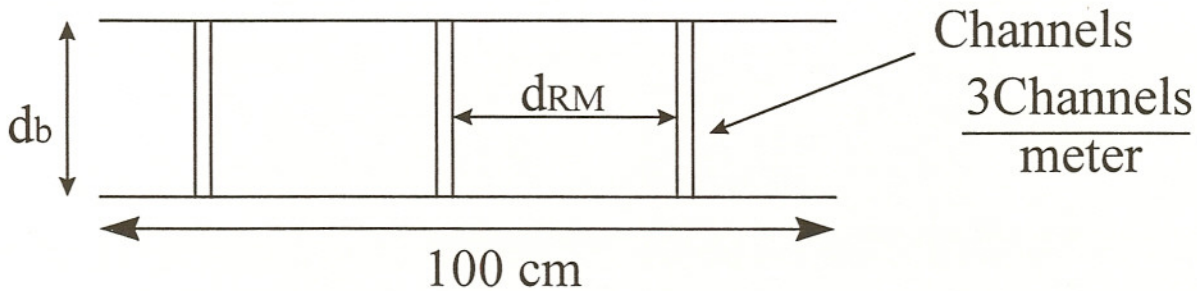


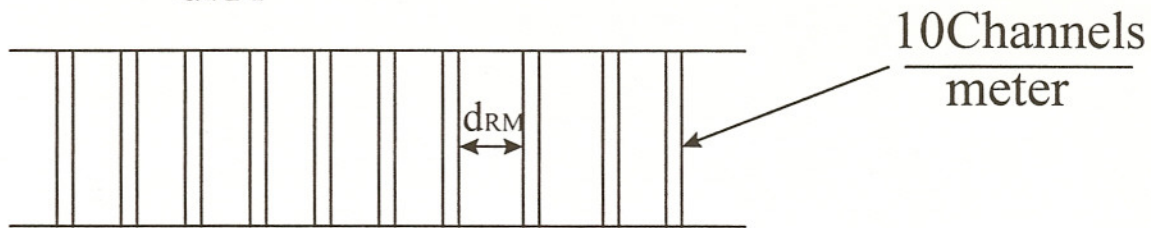
Fig. 21. Contaminant loss as a function of barrier length for different values of  $K_a/K_b$

$$N = \frac{J_{BCH}}{J_B} \sim \left( \frac{d_b}{d_{RM}} \right)^2, d_b = 100\text{cm}$$

$$N = 10, \frac{d_b}{d_{RM}} \sim 3, d_{RM} \sim 30\text{cm}$$



$$N = 100, \frac{d_b}{d_{RM}} \sim 10, d_{RM} \sim 10\text{cm}$$



$$N = 1000, \frac{d_b}{d_{RM}} \sim 30, d_{RM} \sim 3\text{cm}$$

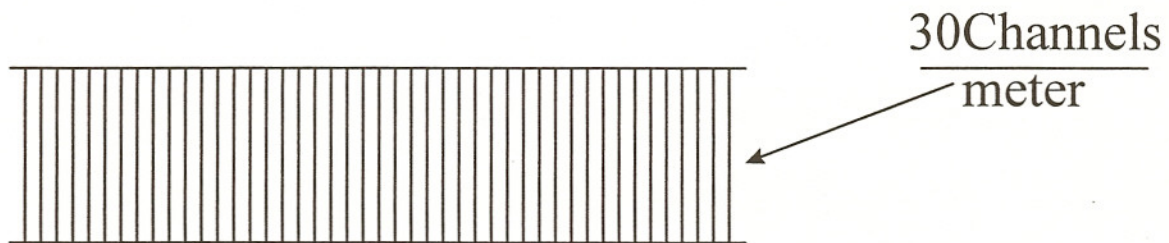


Fig. 22. Number of channels at different hydraulic conductivity magnification